Abstract

Generators driven by axial-flow air-turbine with stator are relatively small in size and can be adapted to withstand violent blizzards. They are suitable for antarctic use, especially as energy sources for unmanned observation units.

An analysis is given of the performance of an axial-flow air-turbine comprising a stator having stationary blades and a rotor having moving blades. Changes in the velocity and thermodynamic properties of the air flow in passing through the turbine are discussed quantitatively, and the expression for the output power and efficiencies of the turbine are given. It is shown that the output attains its maximum when the axial velocity of the air flow in the turbine is $1/\sqrt{3}$ of the wind velocity. The method of evaluation of the maximum annual wind energy available is discussed.

The design of turbine blades is described: the constant nozzle angle design is adopted for the stationary blades, and the axially leaving velocity design for the moving blades. The starting torque, the starting wind velocity, and the off-design performance of the wind air-turbine are also studied. The performance of an air-turbine with stator is compared theoretically to that of an ordinary wind air-turbine without stator, and it is verified the maximum output power allowable for the former will be about 140% of the latter at a lower rotational speed than the latter, which will be about 70% thereof.

A wind electric generator designated NU-101 which has been designed on the basis of the discussion outlined above is described. This comprises an axial-flow air-turbine, 1.2 m in diameter, whose maximum rotational velocity is 300 RPM, and a 2 kW, 100V, AC generator. In 1972, this generator was shipped to Syowa Station, Antarctica, by the 14th Japanese Antarctic Research Expedition (JARE). The results of some test runs in Tokyo in 1972 and at Syowa Station in 1973 are given.

1. Introduction

The consumption of petroleum at Syowa Station, Antarctica, from February 1970 to January 1971 amounted to 266 kl; the petroleum supply by the 12th JARE in February 1970 was 293 tons, which accounted for 64% of the total cargo of the ice-braker FUJI. These figures suggest that the activities at Syowa are likely to be restricted by fuel supply. The situation is much the same with other antarctic stations.

A dormant energy source in the Antarctic is the wind. At Syowa Station, the daily mean wind speed exceeds 10 m/s on 75 days of a year; the yearly mean is 6 m/s, the wind direction being nearly NE throughout the year. At Mizuho Camp (70°42′S, 44°20′E), 300 km inland from Syowa, the yearly mean exceeds 9 m/s, the direction being steadily E or ESE.

The present paper deals with the design of a 2 kW axial-flow air-turbine electric generator constructed in 1972 at the Nihon University, Tokyo, and designated NU-101, for use in these areas. The results of some test runs carried out in Tokyo in 1972 and at Syowa Station in 1973 are described.

2. Requirements to Be Met by Wind Electric Generator for Antarctic Use

The wind may be utilized as an energy source in the Antarctic for two purposes:

(1) To provide a station with an auxiliary electric generator, typically of 5 to 10 kW capacity.

(2) To provide an unmanned observation unit with an electric generator, typically of 30 to 500 W capacity.

The designs of such wind generators are subject to the following requirements:

(1) The rotor diameter should be small, not only because of strength considerations but for convenience of transportation, especially if helicopter transportation is planned. If long blades, such as those of propeller type, are to be employed, they should be detachable.

(2) The wind generator must withstand violent blizzards exceeding 30–60 m/s.

(3) It should have a high efficiency at any wind velocity from 4–5 m/s up to a maximum velocity to be determined.

(4) A safety device is required which prevents the wind generator from rotating unduly fast. The maximum allowable rotating speed is determined by the strength of the rotating parts and the capacity of the electric generator.

(5) The wind generator should be provided with an automatic direction-control device which always keeps the machine axis parallel to the wind, unless the wind direction is steady throughout the year.

3. Outline of Wind Electric Generator NU-101

The ordinary propeller-type wind-turbine having two, three, or four long blades is not always suitable for use in the antarctic field, because of its propeller dimensions. It is a difficult task to reassemble the blades, to erect a tall pole, and to mount the air-turbine on the top of the pole under the antarctic weather. An axial-flow wind air-turbine with stator would seem to be much more promising.

Figs. 1, 2 and 3 illustrate a small wind electric generator, NU-101, which was designed and constructed in 1972 to comply with the requirements described above. This generator, was designed as a prototype of an electric source for use at unmanned observation stations in the Antarctic. The air-turbine has a stator consisting of stationary blades and a rotor having moving blades, both with 1.2 m diameter. The air-turbine is coupled with a 2 kW, single phase,

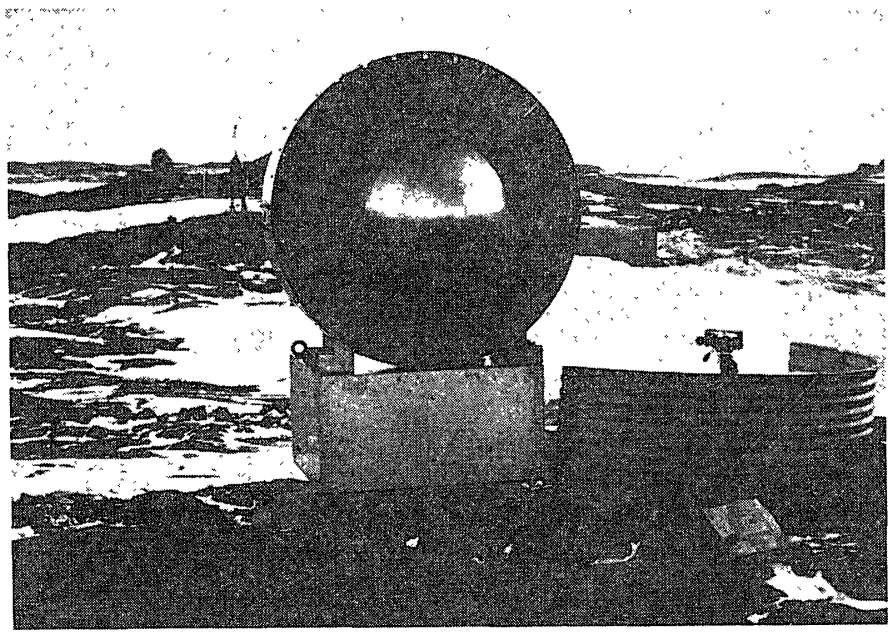

Fig. 1. Axial-flow type wind air-turbine NU-101 (front view) at Syowa Station.

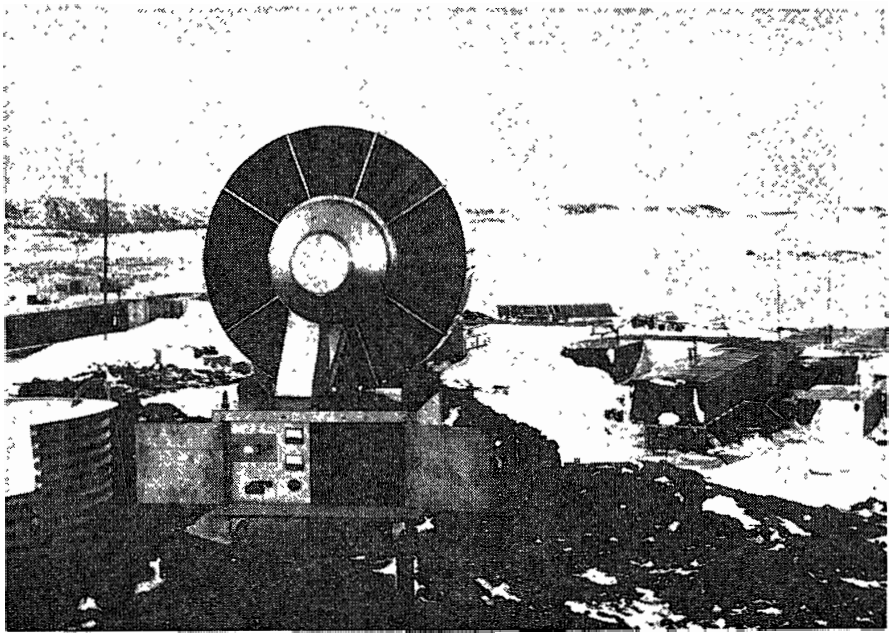

Fig. 2. NU-101 (rear view) at Syowa Station.

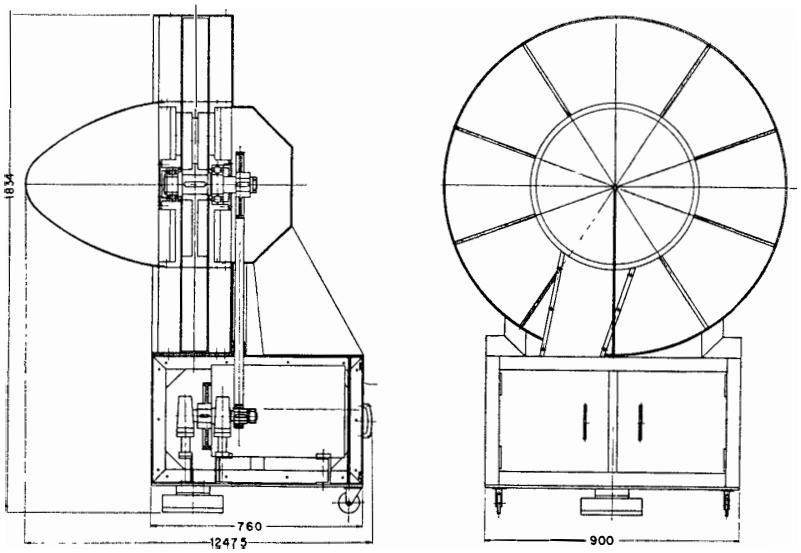

Fig. 3. Sectional view of NU-101.

100V, AC generator through two-step belt-wheel trains (total speed-up ratio being 6:1). The principles of design of this axial-flow air-turbine are given below.

4. Analysis of Performance of Axial-Flow Air-Turbine

4.1. Outline of velocity distribution

Fig. 4 illustrates the air stream flux that passes through a NU-101 type axial-flow air-turbine. Inside such a turbine, the wind velocity has axial and tangential components, which will be designated by suffixes x and y respectively, its radial component being negligible.

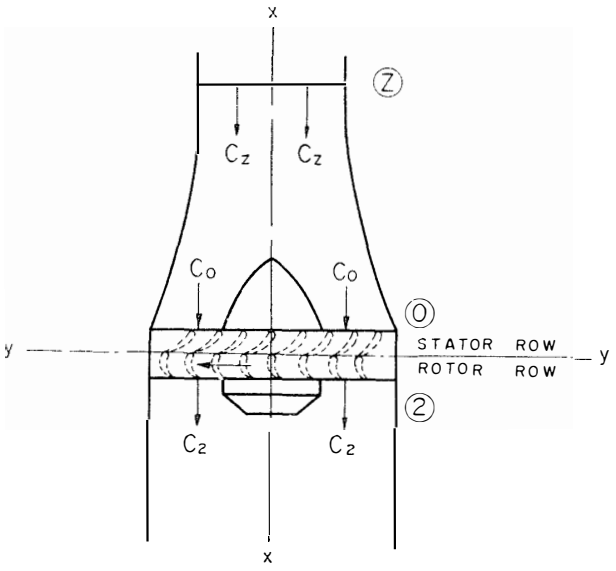

Fig. 4. Air stream flux passing through an axial-flow wind air-turbine.

Let us assume that, at a point Z infinitely distant from the turbine, the wind velocity is parallel to the axis of the turbine (x-x in Fig. 4) and its magnitude is equal to C_z. Let us further assume that this is decreased to C_0 at the entrance to the turbine, with an increase in static pressure from P_z to P_0. The axial component of the velocity inside the turbine, C_x, is assumed to be uniform and equal to C_0 because of a constant cross-sectional passage area and nearly uniform air-density (since the law of conservation of mass flow has to be satisfied).

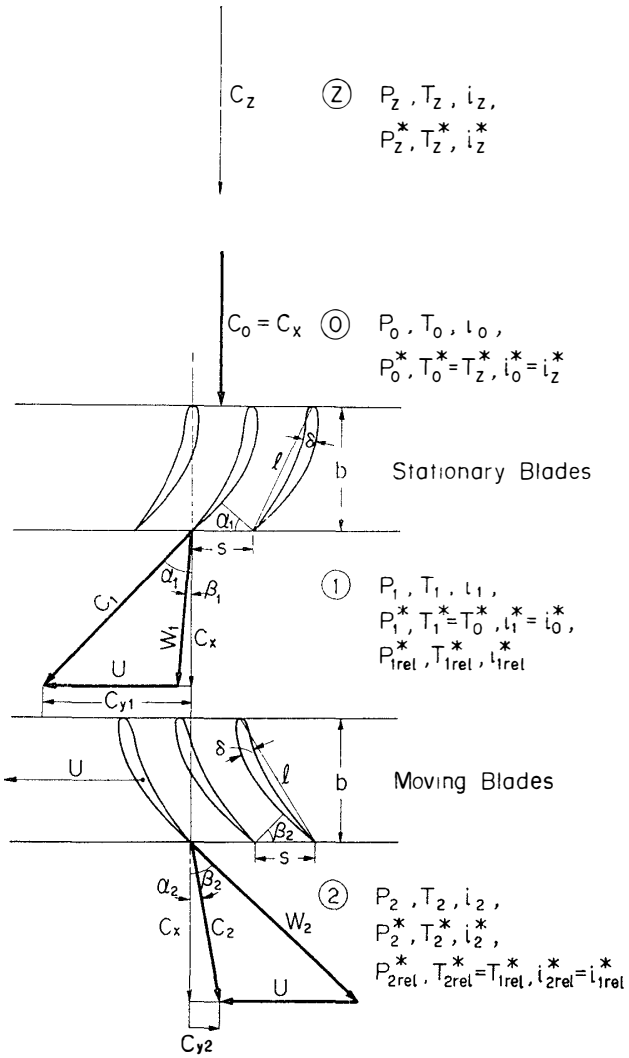

Fig. 5. Stator and rotor rows of an axial-flow air-turbine.

Inside the stator, the air velocity acquires a tangential component in the direction of rotation. Thus the air velocity increases from C_0 to C_1, the exit velocity, being accompanied by a decrease in static pressure from P_0 to P_1 (Figs. 5).

In passing through the rotor, the air stream thrusts the blades in the tangential direction, producing a torque on the output shaft. In a reaction turbine, there is possibility that the air stream will be accelerated relative to the moving blades with reaction torque, resulting in a drop in static pressure from P_1 to P_2 and a drop in static temperature from T_1 to T_2.

4.2. Notations

We shall use the following notations in the analysis of the air stream flux

outlined above. Subscripts Z,0,1 and 2 suffixed to the notation of a quantity indicate that this quantity is measured at a point on the x-axis sufficiently distant from the turbine, just ahead of the stator, at the exit of the stator (entrance of the rotor), and at the exit of the rotor, respectively (see Fig. 5).

(a) Velocities

C	absolute velocity of air relative to earth, m/s.
C_x	wind velocity, m/s.
C_x	axial component of C, m/s.
C_u	tangential component of C, m/s.
C_0	inlet absolute velocity to stator, m/s.
C_1	exit absolute velocity from stator, m/s.
C_2	exit absolute velocity from rotor, m/s.
W	relative velocity of air to rotating rotor, m/s.
W_1	inlet relative velocity to rotor, m/s.
W_2	outlet relative velocity from rotor, m/s.
U	tangential velocity of rotor at radius r, m/s.
U_m	tangential velocity of rotor at mean radius r_m, m/s.

(b) Velocity angles

α_0	angle between C_0 and x-axis, deg.
α_1	angle between C_1 and x-axis, deg.
α_2	angle between C_2 and x-axis, deg.
$\varepsilon_s=\alpha_0+\alpha_1$	deflection angle of stationary blade, deg.
β_1	angle between W_1 and x-axis, deg.
β_2	angle between W_2 and x-axis, deg.
$\varepsilon_m=\beta_1+\beta_2$	deflection angle of moving blade, deg.

(c) Other quantities (for definitions, see 4.3.)

P	static pressure, kg/m^2 or mm H_2O.
P^*	total pressure, kg/m^2 or mm H_2O.
T	static temperature, K.
T^*	total temperature, K.
i	static enthalpy, kcal/kg.
i^*	total enthalpy, kcal/kg.
S	entropy, kcal/kg. K.
c_p	specific heat at constant pressure, kcal/kg. K.
c_v	specific heat at constant volume, kcal/kg. K.
κ	specific heat ratio, $\kappa=c_p/c_v$. $\kappa=1.40$ for air.
R	gas constant, kg. m/kg. K. $R=29.27$ for air.
A	heat equivalent of work, kcal/kg. m. $A=1/426.9$.
g	gravitational acceleration, m/s^2. $g=9.80$.
M	Mach number. $M=C/\sqrt{\kappa gRT}$.
γ	specific weight, kg/m^3.

E_0	maximum value of total wind energy available in a year, kWh/y.
E	maximum value of total indicated energy generated by an air-turbine in a year, kWh/y.
e_0	ideal specific output of air-turbine, kW/m^2.
r_t	tip radius of moving blades, m.
r_h	hub radius of moving blades, m.
r_m	mean radius of moving blades, m.
H	blade height, m. $H=r_t-r_h$.
a	annulus area of a rotor, m^2. $a=\pi(r_t^2-r_h^2)$.
G	weight flow rate of air passing through turbine, kg/s.
D	number of days for a wind velocity C_z per year, days/y.
L_{ti}	indicated output of air-turbine, kW.
L_{te}	brake output of air-turbine, kW.
L_g	net output of generator, kW.
η_{TT}	total-to-total efficiency of air-turbine.
η_{TS}	total-to-static efficiency of air-turbine.
η_g	generator efficiency.
ξ_s	frictional loss coefficient of stationary blades.
ξ_m	frictional loss coefficient of moving blades.
l	chord length of blade, m (see Fig. 5).
S	spacing of blades, m.
δ	maximum thickness of blade, m.
δ/l	thickness ratio.
b	normal chord length, m.
ν	kinematic viscosity of air, m/s^2.
R_h	Reynolds number.
F	normal exit area of a blade, m^2.
φ_s	velocity coefficient of stationary blades.
Φ	flow coefficient, $\Phi=C_x/U$.
Ψ	loading coefficient, $\Psi=\Delta L_{ti}/(U^2/g)$.
ΔL_{ti}	specific indicated output, kg. m/kg.
N	rotational velocity of turbine, RPM.
ω	angular velocity, rad/s.
$d\omega/dt$	angular acceleration, rad/s^2.
t	time, s.
I_p	polar mass moment of inertia of rotating parts, kg. m. s^2.
T_i	indicated torque, kg. m.
T_e	brake torque, kg. m.
T_f	mechanical friction torque, kg. m.
$(T_i)_0$	starting torque, kg. m.
$(C_z)_0$	starting wind velocity, m/s.

4.3. Relations between thermodynamic quantities

The static enthalpy i is defined by

$$i = c_p T \tag{1}$$

where T is the static temperature. The total enthalpy i^* is defined by

$$i^* = i + AC^2/2g = c_p T + AC^2/2g = c_p T^* \tag{2}$$

where

$$T^* = T + AC^2/2gc_p \tag{3}$$

and is called total temperature.

For a perfect gas,

$$c_p = \kappa AR/(\kappa - 1) \tag{4}$$

and mach number is defined as

$$M = C/\sqrt{\kappa g R T}.$$

Hence

$$T^* = T\left[1 + \frac{(\kappa - 1)}{2} M^2\right]. \tag{6}$$

The total enthalpy i^*, and hence the total temperature T^* of any flow confined in a duct or in a free stream flux tube is conserved, *i.e.*,

$$i^* = \text{const.} \tag{7}$$

and

$$T^* = \text{const.} \tag{8}$$

This is true with any fluid flow with or without frictional loss, in so far as neither heat nor external work is added to or taken from the flow.

The total pressure P^* is defined as

$$P^* = P + \gamma C^2/2g. \tag{9}$$

For air, the specific weight γ included in eq. (9) can be calculated as

$$\gamma = 1.293\ (P/1013)\ (273.2/T)\ \text{kg/m}^3 \tag{10}$$

where P (mb) and T (K) are static pressure and static temperature, respectively. The total pressure P^* of any reversible and iso-entropic fluid flow without frictional loss is conserved. *i.e.*,

$$P^* = \text{const.} \tag{11}$$

The total pressure of a fluid flow with frictional loss decreases in the course of its movement. A difference in total pressure which is caused by the frictional loss, is observed between two points located along such flow.

In dealing with a fluid flow passing through the rotor of an air-turbine, we must substitute C included in the expressions for i^*, T^*, and P^*—eqs. (2), (3) and (9)—by W, the velocity relative to the rotor, thereby obtaining

$$i_{rel}^* = i + AW^2/2g \tag{12}$$

$$T_{rel}^* = T + AW^2/2gc_p \tag{13}$$

$$P_{rel}^* = P + \gamma W^2/2g. \tag{14}$$

The total enthalpy (relative) i_{rel}* and the total temperature (relative) T_{rel}* are conserved in such a flow, be it accompanied or unaccompanied by frictional loss, *i.e.*,

$$i_{rel}^* = \text{const.} \tag{15}$$

$$T_{rel}^* = \text{const.} \tag{16}$$

However, the total pressure P_{rel}* is not conserved except in a fluid flow without frictional loss.

The performance of an axial-flow air-turbine can easily be analyzed on the basis of the relations given above.

4.4. Precompression of air in front of an air-turbine

The air speed is reduced from C_z to C_0 before entering into the turbine, and the air is precompressed slightly from the atmospheric pressure P_z to P_0. The deceleration takes places practically unaccompanied by frictional loss. Hence, the following equations can be derived from eqs. (7), (8) and (11).

$$i_z^* = i_z + AC_z^2/2g = i_0^* = i_0 + AC_0^2/2g \tag{17}$$

$$T_z^* = T_0^* \tag{18}$$

$$P_z^* = P_z + \gamma C_z^2/2g = P_0^* = P_0 + \gamma C_0^2/2g \tag{19}$$

and

$$C_z > C_0 = C_x\,, \qquad \alpha_0 = 0\,, \qquad P_z < P_0\,. \tag{20}$$

4.5. Expansion of air in passing through stator

The air flow suffers some frictional loss in passing through the stator. This causes an irreversible expansion. If we compare the states of the air before (0) and after (1) it passes through the stator, we obtain the following relations from eqs. (7) and (8):

$$i_0^* = i_0 + AC_0^2/2g = i_1^* = i_1 + AC_1^2/2g \tag{21}$$

$$T_0^* = T_1^*. \tag{22}$$

The total pressures at (0) and (1) are represented by

$$P_0^* = P_0 + \gamma C_0^2/2g$$

$$P_1^* = P_1 + \gamma C_1^2/2g \tag{24}$$

P_1* is slightly smaller than P_0*, and the difference thereof, ΔP_s* indicates the flow loss of the stationary blades, *i.e.*,

$$\Delta P_s^* = P_0^* - P_1^* = (P_0 - P_1) - \gamma(C_1^2 - C_0^2)/2g\,. \tag{25}$$

Therefore, the absolute velocity increases from C_0 to C_1 at the expense of pressure drop $(P_0 - P_1 - \Delta P_s^*)$, but in all cases, C_1 cannot exceed the original wind velocity C_z, *i.e.*,

$$C_z \geqq C_1 > C_0 = C_x\,. \tag{26}$$

The retarded air at the entrance to the stator, flows into it axially with a velocity C_0 and is accelerated again to an exit velocity C_1 and the direction of the air stream is deflected along the blades to an exit angle α_1, which is nearly equal to the geometrical blade exit angle. The angles between C_0, C_1 and x-axis are defined by α_0 and α_1 respectively. As the air flows into the stator axially, the inlet angle α_0 must be equal to zero, and by referring to Fig. 5, the following relations must be satisfied

$$C_1 \cos \alpha_1 = W_1 \cos \beta_1 = C_x \tag{27}$$

$$C_1 \sin \alpha_1 = C_{y1} . \tag{28}$$

4.6. Air flow passing through rotor

The exit stream from the stator impinges on the moving blades and rotates them with a tangential velocity U at a radius r by consuming its kinetic energy. As shown in Fig. 5, the air stream enters into the moving blades with a relative velocity W_1 and leaves from them with an exit relative velocity W_2. The angles between W_1, W_2 and x-axis are defined by β_1 and β_2, respectively. If we compare the states of the air before (1) and after (2) passing through a rotor, we obtain the following relations from eqs. (12), (13), (15) and (16).

$$i_{1rel}{}^* = i_1 + AW_1{}^2/2g = i_{2rel}{}^* = i_2 + AW_2{}^2/2g \tag{29}$$

$$T_{1rel}{}^* = T_1 + AW_1{}^2/2gc_p = T_{2rel}{}^* = T_2 + AW_2{}^2/2gc_p . \tag{30}$$

These equations show that the total enthalpy (relative) $i_{rel}{}^*$ and the total temperature (relative) $T_{rel}{}^*$ are conserved in the air passing through the rotor. But the total pressure (relative) $P_{rel}{}^*$ is not conserved except in the flow without frictional loss.

The total pressure (relative) at the inlet and at the exit of rotor are given as follows.

$$P_{1rel}{}^* = P_1 + \gamma W_1{}^2/2g \tag{31}$$

$$P_{2rel}{}^* = P_2 + \gamma W_2{}^2/2g \tag{32}$$

and the difference between them is

$$\Delta P_{rel}{}^* = P_{1rel}{}^* - P_{2rel}{}^* = (P_1 - P_2) - \gamma (W_2{}^2 - W_1{}^2)/2g . \tag{33}$$

The total pressure (relative) difference, $\Delta P_{rel}{}^*$, represents the frictional loss of the rotor. Eq. (33) shows us that W_2 will be higher than W_1 when the static pressure difference $(P_1 - P_2)$ is greater than $\Delta P_{rel}{}^*$. In this case, the air will expand in both of stator and rotor, and the stage is usually called "reaction stage". If the air expands only in the stator, and not in the rotor, the stage is referred to as "pure impulse stage".

In the reaction stage, the kinetic energy is supplied to the air not only in the stator, but also in the rotor by the expansion of itself, and some reaction torque is added to the torque due to the impulse of exit air from stator.

The exit absolute velocity C_2 from the rotor is given as a vector sum of W_2 and U as shown in Fig. 5.

The total enthalpy i_2* and the total temperature T_2* are given by

$$i_2^* = i_2 + AC_2^2/2g \tag{34}$$

$$T_2^* = T_2 + AC_2^2/2g\, c_p\,. \tag{35}$$

The angle between the absolute velocity C_2 and x-axis is defined as α_2, which becomes zero when the leaving absolute velocity coincides with the axial velocity C_x. The turbine blade design of this type is usually called an "axially leaving velocity design". In this turbine, the leaving air from the rotor does not have any whirling velocity component. The total pressure P_1* ahead of the rotor is represented by eq. (24), and the total pressure at the exit of the rotor is given by

$$P_2^* = P_2 + \gamma C_2^2/2g \tag{36}$$

P_1* is always greater than P_2* in a turbine. In eq. (36), the static pressure P_2 must be equal to the atmospheric pressure P_z.

By referring to Fig. 5, the following relations are reduced:

$$C_2 \cos\alpha_2 = W_2 \cos\beta_2 = C_x \tag{37}$$

$$C_2 \sin\alpha_2 = C_{y2} \tag{38}$$

and if $\alpha_2 = 0$, from eq. (37) $C_2 = C_x$.

4.7. Graphical representation of air states on *i-s* or *i**-*s* diagram

The working lines of air in an air-turbine are represented graphically on a static enthalpy-entropy diagram (*i-s* diagram) and on a total enthalpy-entropy diagram (*i**-*s* diagram) as shown in Fig. 6. The atmospheric state is represented by a point Z as the cross point of a constant pressure line corresponding to P_z and a horizontal static temperature line T_z. The total state can be determined by a point Z* on the vertical line passing through Z so as to satisfy eq. (17). The constant pressure line through Z* represents the total pressure P_z* shown by eq. (19), and the horizontal line through Z* represents the total enthalpy i_z* and also the total temperature T_z*.

The precompression in the free stream flux is given by a vertical straight line Z-0 in static state and Z* or 0* in total state because of an isoentropic compression. The point 0* coincides with the point Z*, because the total enthalpy and the total temperature are conserved between Z* and 0* as shown by eqs. (17) and (18).

The expansion of air in passing through the stator is represented by a working line 0-1 in static state and a horizontal line 0*-1* in total state, and eqs. (21) and (22) must be satisfied. The difference of total pressure lines P_0* and P_1* shows the loss of stationary blades ΔP_s*.

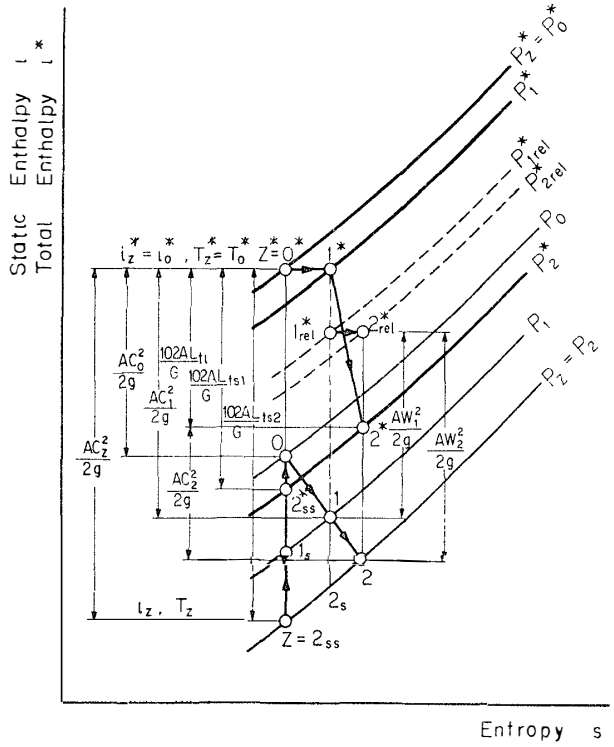

Fig. 6. Working lines of a wind air-turbine on i-s and i-s diagrams of air.*

The expansion of air in passing through the rotor is represented by a working line 1-2 in static state and 1*-2* in total state.

In the expansion, the total enthalpy (relative) i_{rel}^* should be kept constant as shown by eq. (29). Hence, a working line 1_{rel}^*-2_{rel}^* shows a horizontal line passing through a point 1_{rel}^*, which is determined on a vertical line passing through point 1 so as to satisfy eq. (29).

The difference of total pressure (relative) lines P_{1rel}^* and P_{2rel}^* gives the flow loss of the moving blades, ΔP_{rel}^*, shown by eq. (33).

In a reaction stage, the static pressure drops from P_1 to P_2, which is equal to the atmospheric pressure P_z.

But in an impulse stage, P_1 should be equal to $(P_z + \Delta P_{rel}^*)$, and P_2 is equal to P_z.

4.8. Output power and efficiencies of air-turbine

The indicated output of a real air-turbine, that contains the effect of frictional loss of flow but not of mechanical friction, is given by the following relation (refer to Fig. 6).

$$L_{ti} = G(i_1^* - i_2^*)/102A = 4.19G(i_1^* - i_2^*)$$
$$= 4.19G(i_z^* - i_2^*) \quad \text{kW} \tag{39}$$

where

$$i_1^*=i_1+AC_1^2/2g,\ i_2^*=i_2+AC_2^2/2g,\ i_z^*=i_z+AC_z^2/2g\ ,$$

and G (kg/s) is the weight flow rate of air through the turbine.

For an ideal, reversible and isoentropic turbine, the inlet state is represented in Fig. 6 by point Z^* in the total enthalpy-entropy (i^*-s) diagram; the exit state from the turbine is represented by 2_{ss}^* in the total enthalpy diagram and by 2_{ss} in the static enthalpy-entropy (i-s) diagram. As the output of such an ideal turbine, the following two kinds of output are defined;

$$L_{ts1}=4.19\mathrm{G}(i_z^*-i_{2ss}^*)\quad \mathrm{kW} \tag{40}$$

$$L_{ts2}=4.19G(i_z^*-i_{2ss})\quad \mathrm{kW} \tag{41}$$

and the following two kinds of efficiencies are defined for a real turbine with blade losses.

$$\text{total-to-total efficiency}:\quad \eta_{TT}=\frac{L_{ti}}{L_{ts1}}=\frac{i_z^*-i_2^*}{i_z^*-i_{2ss}^*} \tag{42}$$

$$\text{total-to-static efficiency}:\quad \eta_{TS}=\frac{L_{ti}}{L_{ts2}}=\frac{i_z^*-i_2^*}{i_z^*-i_{2ss}} \tag{43}$$

It can be easily shown that

$$\eta_{TS}/\eta_{TT}=1-(\mathrm{C}_2/C_z)^2\ . \tag{44}$$

For an ideal turbine with no frictional loss in flow,

$$\eta_{TT}=1\quad\text{and}\quad \eta_{TS}=1-(C_2/C_z)^2<1\ . \tag{45}$$

For a real turbine with frictional loss in flow,

$$\eta_{TT}<1\ ,\qquad \eta_{TS}=\eta_{TT}[1-(C_2/C_z)^2]<\eta_{TT}\ . \tag{46}$$

From eq. (42), it follows that

$$L_{ti}=\eta_{TT}L_{ts1}=\frac{\eta_{TT}G}{102A}(i_z^*-i_{2ss}^*)=\frac{\eta_{TT}G}{102\times 2g}(C_z^2-C_2^2)\ .$$

Thus

$$L_{ti}=\frac{\eta_{TT}G}{2000}(C_z^2-C_2^2)\quad \mathrm{kW} \tag{47}$$

or

$$L_{ti}=\frac{\eta_{TS}G}{2000}C_z^2\qquad \mathrm{kW} \tag{48}$$

Eqs. (47) and (48) can conveniently be employed in evaluating the indicated output of a real air-turbine.

4.9. Flow rate of air and ideal specific output

The weight flow rate G of air passing through the annulus area between r_h (hub radius) and r_t (tip radius) of an air-turbine is given by

$$G=2\pi\gamma\int_{r_h}^{r_t} C_x r dr \quad \text{kg/s} \tag{49}$$

and the annulus area a is given by

$$a=\pi(r_t^2-r_h^2) \quad \text{m}^2. \tag{50}$$

When the axial velocity C_x is uniform along radius, eq. (49) can be reduced to

$$G=\gamma a C_x \quad \text{kg/s}. \tag{51}$$

It is usual in those air-turbines which are provided with long blades that the axial velocity C_x varies as a function of radial distance r from the central axis. In such a case, G should be calculated from eq. (49) or from eq. (51), in which C_x should be replaced by its mean value C_{xm}.

With an axially leaving velocity design, the absolute exit velocity C_2 has no tangential component and the exit angle

$$\alpha_2=0 \tag{52}$$

(see Fig. 5), hence

$$C_2=C_{xm}. \tag{53}$$

The indicated output of such an air-turbine is, according to eqs. (47), (51), and (53)

$$L_{ti}=\frac{\eta_{TT}\gamma a}{2000}C_{xm}(C_z^2-C_{xm}^2) \quad \text{kW} \tag{54}$$

$$L_{ti}=\frac{\eta_{TT}\gamma a}{2000}C_{xm}^3[(C_z/C_{xm})^2-1] \quad \text{kW} \tag{55}$$

The output becomes maximum when

$$\frac{\partial L_{ti}}{\partial C_{xm}}=0$$

By differentiating eq. (54), we get

$$C_{xm}=C_z/\sqrt{3} \tag{56}$$

and the maximum indicated output $L_{ti,\max}$ is

$$L_{ti,\max}=\frac{\eta_{TT}\gamma a}{1000}\frac{C_z^3}{3\sqrt{3}} \quad \text{kW}. \tag{57}$$

Thus the maximum indicated output of an ideal air-turbine without frictional loss per unit area of the annulus, or the ideal specific output, e_0, is given by

$$e_0=\frac{L_{ti,\max}}{a\eta_{TT}}=\frac{\gamma}{1000}\frac{C_z^3}{3\sqrt{3}} \quad \text{kW/m}^2. \tag{58}$$

Table 1 gives the values of e_0 together with those of

$$G/a=\gamma C_z/\sqrt{3} \quad \text{kg/s.m}^2 \tag{59}$$

for various values of the wind velocity C_z. By the use of this table, one may easily estimate the maximum attainable output at a given wind velocity of an axial-flow air-turbine. Note, however, that the values in Table 1 have been calculated by assuming γ to be 1.293 kg/m^3. If this is not the case, one must

Table 1. Specific output e_0 and specific weight flow G/a for an axial-flow air-turbine ($\eta_{TT}=1$, $\gamma=1.293$ kg/m³).

C_z (m/s)	e_0 (kW/m²)	G/a (kg/s.m²)	C_z (m/s)	e_0 (kW/m²)	G/a (kg/s.m²)	C_z (m/s)	e_0 (kW/m²)	G/a (kg/s.m²)
0		0	20	1.990	14.93	40	15.67	29.86
1	0.00025	0.747	21	2.304	15.68	41	16.87	30.61
2	0.00199	1.493	22	2.649	16.42	42	18.14	31.35
3	0.00672	2.239	23	3.027	17.17	43	19.46	32.10
4	0.0159	2.986	24	3.499	17.92	44	20.85	32.85
5	0.0311	3.733	25	3.888	18.66	45	22.31	33.59
6	0.0537	4.479	26	4.373	19.41	46	23.82	34.34
7	0.0853	5.226	27	4.897	20.16	47	25.42	35.09
8	0.1274	5.972	28	5.462	20.90	48	27.07	35.83
9	0.1814	6.718	29	6.317	21.65	49	28.80	36.58
10	0.2488	7.465	30	6.718	22.40	50	30.60	37.33
11	0.3312	8.212	31	7.412	23.14	51	32.47	38.07
12	0.4299	8.958	32	8.153	23.89	52	34.42	38.82
13	0.5466	9.705	33	8.941	24.64	53	36.45	39.57
14	0.6827	10.45	34	9.779	25.38	54	38.55	40.31
15	0.8397	11.20	35	10.49	26.13	55	40.73	41.06
16	1.019	11.94	36	11.42	26.88	56	42.99	41.81
17	1.222	12.69	37	12.40	27.62	57	45.34	42.55
18	1.451	13.44	38	13.43	28.37	58	47.76	43.30
19	1.707	14.18	39	14.52	29.11	59	50.28	44.05
20	1.990	14.93	40	15.67	29.86	60	52.88	44.79

multiply the table values by $(\gamma/1.293)$, where γ is the actual specific weight of the air which is to be calculated according to eq. (10).

Let us assume that there are D days in a year on which the daily mean wind velocity is equal to C_z. We may then calculate the maximum total wind energy per year per unit area of the annulus that can be obtained from winds of velocity C_z as

$$(E_0/a)=24De_0 \quad \text{kWh/y}\cdot\text{m}^2 . \tag{60}$$

Here e_0 can be obtained from eq. (58) or from Table 1.

The total wind energy available in a year per unit area of the annulus of an air-turbine can be calculated by

$$\sum_{C_z}(E_0/a)=\sum_{C_z}(24De_0) \quad \text{kWh/y}\cdot\text{m}^2 \tag{61}$$

and the total indicated energy generated by a real air-turbine with an annulus area a through one year, E, is given by

$$E=\eta_{TT}a\sum_{C_z}(E_0/a) \quad \text{kWh/y} \tag{62}$$

if the total-to-total efficiency η_{TT} of the air-turbine is independent of C_z.

As an example, the number of days D for any daily-mean wind velocity C_z at Syowa Station in 1970 is given in Table 2 (JAPAN METEOROLOGICAL AGENCY, 1971).

Table 3 shows the total energy that can be generated in a year by an ideal air-turbine ($\eta_{TT}=1$) with the annulus area $a=1\text{m}^2$ at Syowa Station. As shown in Fig. 7 and Table 3, the value of (E_0/a) becomes a maximum at a wind velocity of $C_z=17$ m/s. Hence, the air-turbine to be used at Syowa Station should be so designed as to exhibit the highest efficiency at wind velocities around 17 m/s. We know that the maximum available total wind energy and yearly mean wattage at Syowa Station for every unit annulus area of air-turbine are less than 1958 kWh/y.m^2 and 223 W/m^2, respectively.

This method will be useful for estimating the maximum available energy generated by a wind air-turbine to be installed in any place from the daily mean wind velocity data observed throughout one year.

Table 2. Number of days D for which daily-mean wind velocity is C_z at Syowa Station in 1970.

C_z m/s	0–2	2–4	4–6	6–8	8–10	10–12	12–14	14–16	16–18	18–20	20–22	22–24	24–26	26–28
January	5	9	10	5	2	0	0	0	0	0	0	0	0	0
February	7	9	3	5	1	0	2	1	0	0	0	0	0	0
March	8	10	4	1	3	1	2	2	0	0	0	0	0	0
April	3	6	5	2	3	4	2	1	1	1	1	0	1	0
May	10	4	1	3	3	2	1	2	2	1	2	0	0	0
June	6	8	1	3	3	5	0	0	2	1	1	0	0	0
July	5	6	6	3	3	2	1	2	2	1	0	0	0	0
August	12	3	5	4	2	2	1	1	0	0	0	0	1	0
September	8	10	5	2	3	0	1	0	1	0	0	0	0	0
October	6	3	5	3	3	1	5	1	2	1	0	1	0	0
November	12	6	3	2	1	2	2	0	1	1	0	0	0	0
December	13	8	3	0	2	1	3	1	0	0	0	0	0	0
Sum D	95	82	51	33	29	20	20	11	11	6	4	1	2	0
%	26.0	22.5	14.0	9.0	8.0	5.5	5.5	3.0	3.0	1.6	1.1	0.3	0.5	0
Sum %	48.5		51.5											
Remarks	Not available		Available zone											

Data obtained from "Meteorological Data at the Syowa Station in 1970" (JAPAN METEOROLOGICAL AGENCY, 1971).

Table 3. Total energy that can be generated in a year by an ideal air-turbine at Syowa Station.

C_z	e_0 (kW/m²)	D (days/y)	E_0/a (kWh/y.m²)	$\sum_{C_z}(E_0/a)$ (kWh/y.m²)	(G/a) (kg/s.m²)
1	0.00025	95	0.58	0.58	0.76
3	0.00679	82	13.4	14.0	2.26
5	0.0314	51	38.4	52.4	3.77
7	0.0862	33	68.3	120.7	5.28
9	0.1834	29	128	249	6.79
11	0.3348	20	160	409	8.30
13	0.5525	20	265	674	9.81
15	0.8488	11	224	898	11.32
17	1.235	11	326	1224	12.83
19	1.725	6	248	1472	14.33
21	2.329	4	224	1696	15.85
23	3.060	1	73	1769	17.36
25	3.930	2	189	1958	18.86

Remarks: e_0 and (G/a) have been corrected for $\gamma = 1.307$ kg/m³.

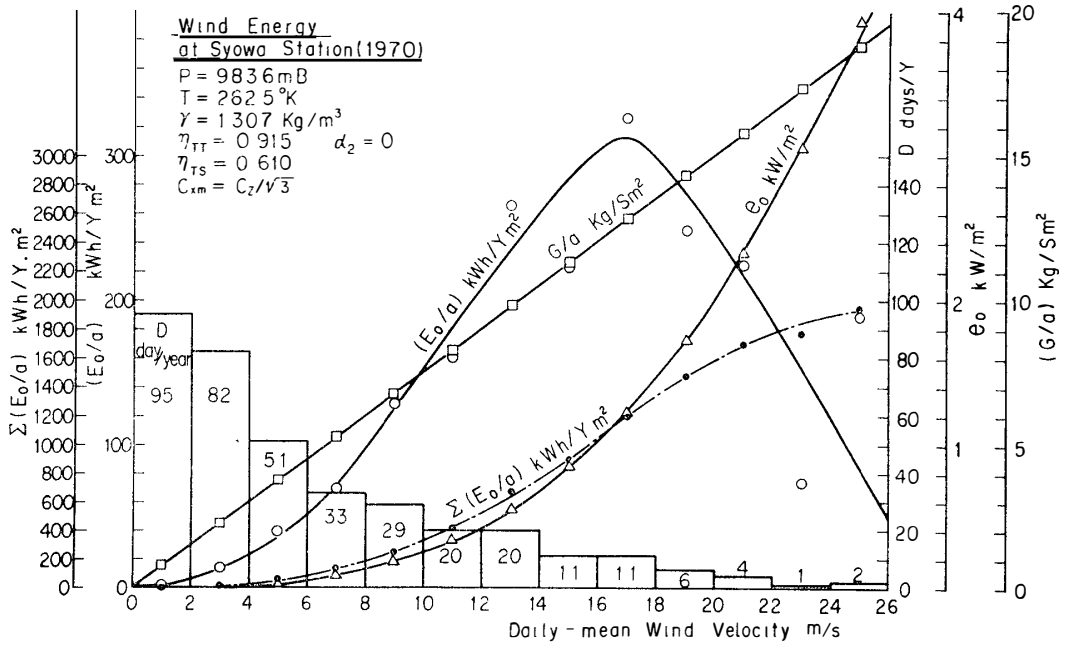

Fig. 7. Wind energy at Syowa Station (1970).

4.10. Estimation of air-turbine efficiencies

As shown above, two kinds of turbine efficiencies are defined by eqs. (42) and (43). These efficiencies of an air-turbine should be obtained by experiments, but in designing a turbine, it is necessary to estimate its efficiencies. For this purpose, SODERBERG's correlation (SODERBERG, 1949; HORLOCK, 1966) for turbine blade losses may be useful.

By referring to Fig. 6 and eq. (42), the total-to-total efficiency η_{TT} can be rewritten as

$$\eta_{TT}=\frac{i_z^*-i_2^*}{i_z^*-i_{2ss}^*}=\frac{i_z^*-i_2^*}{(i_z^*-i_2^*)+(i_2^*-i_{2ss}^*)}$$
$$=\frac{1}{1+(i_2^*-i_{2ss}^*)/(i_z^*-i_2^*)}=\frac{1}{1+\zeta} \tag{63}$$

where

$$\zeta=\frac{i_2^*-i_{2ss}^*}{i_z^*-i_2^*}\,. \tag{64}$$

In these equations, $(i_2^*-i_{2ss}^*)$ represents the sum of the frictional losses of stationary and moving blades and is expressed as

$$i_2^*-i_{2ss}^*=i_2-i_z=\xi_s(AC_1^2/2g)+\xi_m(AW_2^2/2g) \tag{65}$$

where ξ_s and ξ_m represent the frictional loss coefficient of the stationary blade and the moving blade, respectively.

In eq. (64),

$$i_z^*-i_2^*=(i_z-i_2)+A(C_z^2-C_2^2)/2g$$
$$=A[(C_z^2-C_2^2)-(\xi_sC_1^2+\xi_mW_2^2)]/2g \tag{66}$$

From eqs. (64), (65) and (66)

$$\zeta=(\xi_sC_1^2+\xi_mW_2^2)/[(C_z^2-C_2^2)-(\xi_sC_1^2+\xi_mW_2^2)]\,. \tag{67}$$

By substituting ζ into eq. (63), the total-to-total efficiency η_{TT} can be calculated, and accordingly, the total-to-static efficiency η_{TS} can be obtained by using eq. (44).

The loss coefficient ξ has been correlated by SODERBERG by referring to many experimental data on the basis of Reynolds number R_h, aspect ratio b/H (where b is the axial chord and H is the blade height), thickness ratio δ/l (where δ is the maximum thickness of the blade and l is the chord length), and deflection angle ε of the blade ($\varepsilon_s=\alpha_0+\alpha_1$ for a stationary blade and $\varepsilon_m=\beta_1+\beta_2$ for a moving blade).

SODERBERG's correlation for the loss coefficient of a turbine blade has been represented as (SODERBERG, 1949; HORLOCK, 1966)

$$\xi=(10^5/R_h)^{1/4}[(1+\xi')(0.975+0.075\,b/H)-1] \tag{68}$$

where ξ' is given by SODERBERG as a graph of $\xi'-\varepsilon$, which is represented by the present authors as follows:

$$\xi'=0.062-0.10(\delta/l)+0.065\times10^{-4}\varepsilon^2\,. \tag{69}$$

In eq. (68), Reynolds number R_h has been defined as

$$R_h=(4F/\text{perimeter})\ (\text{exist velocity})/(\text{kinematic viscosity } \nu) \quad (70)$$

where F is the normal exit area of a flow channel (see Fig. 8), and perimeter means the perimeter of the same exit area. Hence, R_h can be calculated by

$$R_h=\left(\frac{2HS\cos\alpha_1}{S\cos\alpha_1+H}\right)C_1/\nu$$

for stationary blades (71)

$$R_h=\left(\frac{2HS\cos\beta_2}{S\cos\beta_2+H}\right)W_2/\nu$$

for moving blades. (72)

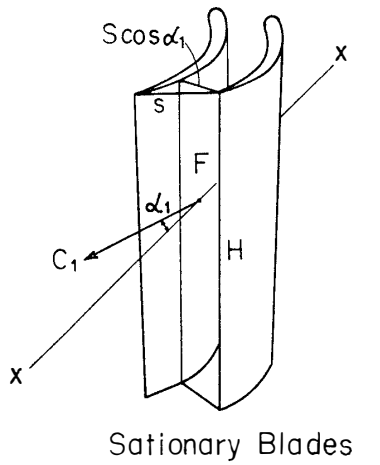

Fig. 8. Normal exit area and its perimeter between two stationary blades.

The kinematic viscosity ν of the air can be calculated by

$$\nu=(0.138+0.009\,t)\times10^{-4}\ \text{m/s}^2 \quad (73)$$

where t is the air temperature in °C.

5. Design of Air-Turbine Blades

As shown by eq. (47), the indicated output of an air-turbine is proportional to G, the weight flow rate of air passing through it, and to $(C_z^2-C_2^2)$, and the output becomes maximum when the mean axial velocity C_{xm} is designed to be $C_z/\sqrt{3}$, where C_z is wind velocity. For maximizing $(C_z^2-C_2^2)$, the exit absolute velocity C_2 must be minimized. The minimum value of C_2 is obtained when it is equal to C_{xm} and this means that the exit angle α_2 is zero.

For this reason, the authors adopted the axially leaving velocity design for the moving blade of NU-101 and the mean axial velocity C_{xm} satisfying eq. (56).

To increase the output power for this limited C_{xm}, the annulus area a must be increased. This results in a low boss ratio r_h/r_t and high blade height H. In this case, there will be a large variation of blade velocity along its radius r so that the designer cannot base his designs on one section and ignore variation in flow conditions with radius r.

Some classical methods of design are known for such long blades based on the radial equilibrium theory (HORLOCK, 1966). The basic assumption of the radial equilibrium theory is that the radial velocity component C_r equals zero, and the static pressure gradient along the radius is in equilibrium with the centrifugal force acting on a mass element at r (see Fig. 9), *i.e.*,

$$\frac{dP}{dr}=\frac{\gamma}{g}\left(\frac{C_y^2}{r}\right). \tag{74}$$

As indicated in eq. (2), the total enthalpy i^* is defined by

$$\begin{aligned} i^* &= i+AC^2/2g \\ &= i+A(C_x^2+C_y^2)/2g \end{aligned} \tag{75}$$

The GIBB's relation derived from the second law of thermodynamics is as follows.

$$T\,ds=d\,i-A\,dP/\gamma \tag{76}$$

From eqs. (74), (75) and (76)

$$\begin{aligned} \frac{di^*}{dr}-T\frac{ds}{dr} &= A\left[\frac{1}{\gamma}\frac{dP}{dr}+\frac{d}{dr}(C_x^2+C_y^2)/2g\right] \\ &= \frac{A}{g}\left[\frac{C_y^2}{r}+\frac{d}{dr}(C_x^2+C_y^2)/2\right]. \end{aligned} \tag{77}$$

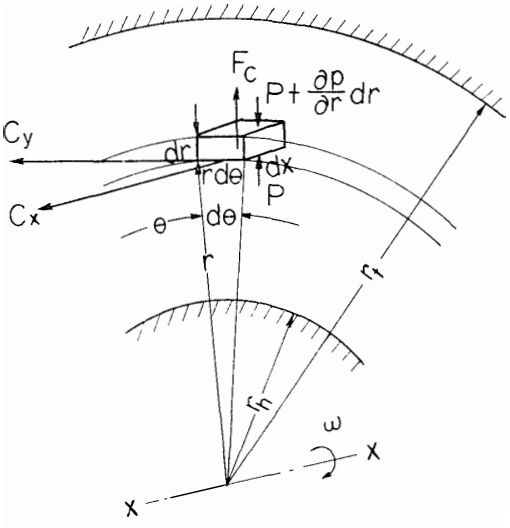

$$F_C = \frac{\gamma}{g}(r d\theta \cdot dx \cdot dr)\frac{C_y^2}{r} = -\frac{\partial p}{\partial r}\, dr(dx \cdot r d\theta)$$

F_C = Centrifugal Force Acting on A Rotating Mass Element

Fig. 9. Radial equilibrium of air flowing through long blades.

For design purposes, it is usually assumed that the total enthalpy i^* and entropy s are constant along the radius, as at entry to the stage.
Hence,

$$\frac{di^*}{dr}=0 \quad \text{and} \quad \frac{ds}{dr}=0\,.$$

With this assumption, the following simplified radial equilibrium equation is obtained from eq. (77)

$$\frac{d}{dr}(C_x^2)+\frac{1}{r^2}\frac{d}{dr}(rC_y)^2=0 \tag{78}$$

which can be rewritten to

$$\frac{d}{dr}(C^2)+\frac{2}{r}C_y^2=0\,. \tag{79}$$

The authors adopted the constant nozzle angle design for the stationary blades of NU-101; that means α_0 and α_1 are kept constant at any radius so that the stationary blades may be straight in radial direction, but the moving blades should be twisted along their radii so as to satisfy eq. (79) and the condition of axially leaving velocity, *i.e.,* the exit angle α_2 is zero, at any radius.

As the air stream flowing into the stator is parallel to the axis of rotation at any radius,

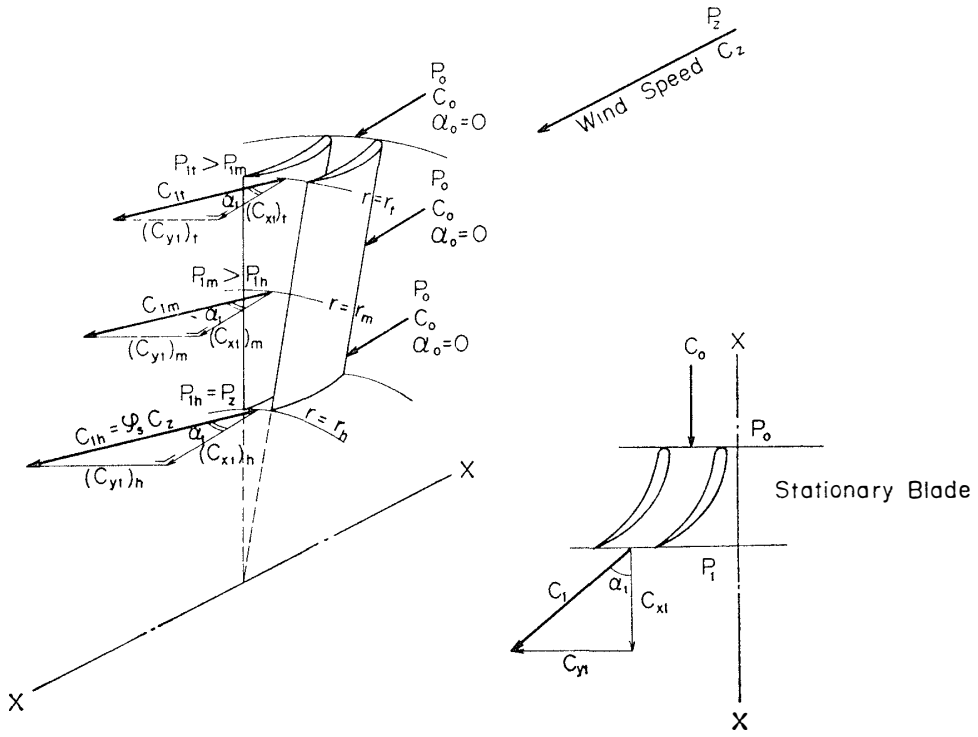

Fig. 10. Constant nozzle angle design ($\alpha_0=0$ and $\alpha_1=$const. at any radius) for the stationary blades.

$$\alpha_0=0, \quad C_0=C_x, \quad C_{y0}=0 .$$

Referring to the exit velocity triangle for the stator (Fig. 10).

$$C_{x1}=\cot\alpha_1 C_{y1} .$$

When the exit angle of C_1 is kept constant along any radius r,

$$d(C_{x1}^2)=\cot^2\alpha_1 d(C_{y1}^2) .$$

Hence

$$d(C_1^2)=d(C_{x1}^2)+d(C_{y1}^2)=(1+\cot^2\alpha_1)d(C_{y1}^2) \tag{80}$$

$$=\operatorname{cosec}^2\alpha_1 d(C_{y1}^2) . \tag{81}$$

From eqs. (79) and (81), we get

$$\frac{1}{2}\operatorname{cosec}^2\alpha_1 \frac{d(C_{y1}^2)}{C_{y1}^2}=-\frac{dr}{r} \tag{82}$$

and

$$rC_{y1}^{\operatorname{cosec}^2\alpha_1}=\text{const} . \tag{83}$$

or

$$C_{y1}=K_1 r^{-\sin^2\alpha_1} \tag{84}$$

$$C_{x1}=K_1(\cot\alpha_1)r^{-\sin^2\alpha_1} \tag{85}$$

$$C_1=K_1(\operatorname{cosec}\alpha_1)r^{-\sin^2\alpha_1} \tag{86}$$

where K_1 is a constant. Eqs. (84), (85) and (86) show that C_{y1}, C_{x1} and C_1

decrease, and accordingly the static pressure P_1 increases, with increase of radius r. The maximum velocity of C_1 is obtained at the hub radius r_h and the velocity is noted as C_{1h}, which is related to the wind velocity C_z as follows:

$$C_{1h} = \varphi_s C_z. \tag{87}$$

Here φ_s is the velocity coefficient of the stationary blade, which is slightly smaller than and nearly equal to 1. It happens in the same case that the static pressure P_{1h} at the hub radius r_h becomes a minimum, which is nearly equal to P_z.

Using the subscripts t, h and m to designate the values at the tip radius, hub radius and mean radius, respectively, we may write according to eqs. (85) and (87)

$$\begin{aligned}(C_{x1})_h &= (C_{x1})_m (r_m/r_h)^{\sin^2\alpha_1} \\ &= C_{1h}\cos\alpha_1 = \varphi_s C_z \cos\alpha_1\end{aligned}$$

Substituting eq. (56) for $(C_{x1})_m$, we obtain

$$(r_m/r_h)^{\sin^2\alpha_1} = \sqrt{3}\,\varphi_s \cos\alpha_1 . \tag{88}$$

The values of the constant nozzle angle α_1 calculated according to eq. (88) for $\varphi_s = 1$ are given in Table 4 for various values of r_m/r_h or r_t/r_h. This is an important equation for determining the constant exit angle α_1 from the stationary blades.

The real value of φ_s of the stationary blades with frictional loss can be obtained as follows:

From eq. (87) and $AC_z^2/2g = (AC_{1h}^2/2g) + \xi_s(AC_{1h}^2/2g)$

$$\varphi_s = 1/\sqrt{1+\xi_s} . \tag{89}$$

Table 4. Constant-cut angle α_1 calculated by eq. (88).

r_m/r_h	r_t/r_h	α_1
1.3	1.6	48.1°
1.4	1.8	46.5°
1.5	2.0	45.0°
1.6	2.2	43.8°
1.7	2.4	42.5°

6. Indicated, Frictional and Brake Torque of an Air-Turbine

If the distribution of the tangential components of absolute velocity along the radius of moving blades is known, the indicated torque may be obtained as the angular momentum change between inlet and outlet (see Fig. 11) in which subscript m indicates the values at mean radius r_m.

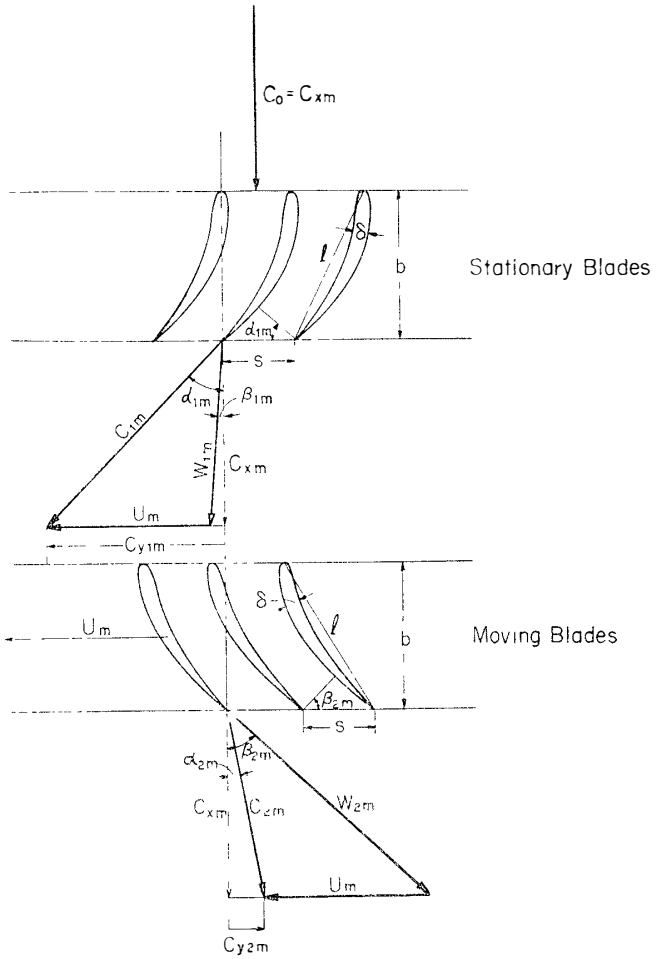

Fig. 11. Velocity triangles at mean radius.

$$\text{Indicated torque } T_i = \frac{G}{g}(C_{y1m} + C_{y2m})r_m \tag{90}$$

$$= \frac{G}{g}C_{xm}(\tan \alpha_{1m} + \tan \alpha_{2m})r_m \tag{91}$$

$$= \frac{G}{g}(C_{1m} \sin \alpha_{1m} + C_{2m} \sin \alpha_{2m})r_m \,. \tag{92}$$

In a general case, an air-turbine must be provided with a speed-up gear box and bearings for supporting the rotor. According, some frictional torque T_f must be overcome. In a transition state, such as acceleration or deceleration of the turbine rotor, inertia torque therefore must be added thereto.

Hence the brake torque T_e driving an electric generator can be expressed by

$$T_e = T_i - T_f \pm I_p \frac{d\omega}{dt} \tag{93}$$

$(-)$: for acceleration

$(+)$: for deceleration

where T_f: mechanical frictional torque of bearings, speed-up gears, and of an electrical generator, kg. m

I_p: polar mass moment of inertia of rotating parts, kg.m.s^2

$\frac{d\omega}{dt}$: angular accelereration, rad/s^2.

In an equilibrium state, the last inertia torque in eq. (93) can be neglected.

The indicated, brake output power of an air-turbine may be calculated as follows.

$$\text{indicated output power } L_{ti} = \frac{2\pi NT_i}{60 \times 102} = \frac{2\pi NT_i}{6120} \text{ kW} \tag{94}$$

$$\text{brake output power } L_{te} = \frac{2\pi NT_e}{60 \times 102} = \frac{2\pi NT_e}{6120} \text{ kW} \tag{95}$$

The total-to-static efficiency can be calculated by

$$\eta_{TS} = \frac{102L_{ti}}{GC_z^2/2g} = 2000\frac{L_{ti}}{GC_z^2} \tag{96}$$

7. Starting Torque and Starting Wind Velocity

The minimum starting torque $(T_i)_0$ necessary for starting a stationary wind air-turbine can be determined from eq. (93) as follows:

$$T_e=0, \quad (T_i)_0=T_f+I_p\frac{d\omega}{dt}. \tag{97}$$

Substituting eq. (91) in this equation, we obtain

$$\frac{G}{g}C_{xm}(\tan\alpha_{1m}+\tan\alpha_{2m})r_m=T_f+I_p\frac{d\omega}{dt} \tag{98}$$

When the mean axial velocity C_{xm} is adopted so as to satisfy eq. (56), the minimum wind velocity $(C_z)_0$ necessary for starting a wind air-turbine can be determined by substituting eqs. (51) and (56) into eq. (98).

$$(C_z)_0=\sqrt{\frac{3g[T_f+I_p(d\omega/dt)]}{\gamma a(\tan\alpha_{1m}+\tan\alpha_{2m})r_m}} \tag{99}$$

For the estimation of the minimum starting wind velocity $(C_z)_0$, the frictional torque T_f and the inertia torque $I_p(d\omega/dt)$ must be obtained experimentally.

On the contrary, when the starting wind velocity $(C_z)_0$ of a wind air-turbine is measured by experiments, the starting torque $(T_i)_0$, the sum of frictional, and inertia torques of the turbine can be easily calculated by the following equation:

$$(T_i)_0=T_f+I_p\left(\frac{d\omega}{dt}\right)=\frac{\gamma a(C_z)_0^2}{3g}(\tan\alpha_{1m}+\tan\alpha_{2m})r_m \tag{100}$$

8. Off-Design Performance of Wind Air-Turbine

In an air-turbine, the performance not only at a design point but the performance at any off-design point is of vital importance because the wind velocity C_z varies greatly.

In order to discuss such off-design performance, we first define the mean flow coefficient, Φ_m and the mean loading coefficient Ψ_m as follows:

$$\Phi_m = C_{xm}/U_m \tag{101}$$

$$\Psi_m = \Delta L_{ti}/(U_m{}^2/g)\,. \tag{102}$$

Here ΔL_{ti} represents the specific indicated output, *i.e.*, the indicated output per 1 kg/s of air flow, and is given by

$$\begin{aligned}\Delta L_{ti} &= 102 L_{ti}/G = T_i\omega/G \\ &= r_m\omega(C_{y1m}+C_{y2m})/g \\ &= U_m C_{xm}(\tan\alpha_{1m}+\tan\alpha_{2m})/g\end{aligned} \tag{103}$$

On the other hand, the following relation must be satisfied in a velocity triangle for moving blades (Fig. 11):

$$C_{xm}\tan\alpha_{2m} = C_{xm}\tan\beta_{2m} - U_m$$

hence,

$$\tan\alpha_{2m} = \tan\beta_{2m} - (1/\Phi_m)\,. \tag{104}$$

From eqs. (102), (103) and (104), we obtain the following relation:

$$\Psi_m = (\tan\alpha_{1m}+\tan\beta_{2m})\Phi_m - 1\,. \tag{105}$$

When the wind velocity C_z varies from a design velocity to any other velocity, the axial velocity C_{xm}, peripheral velocity U_m at mean radius r_m, and accordingly Φ_m, vary from those for a design point. Even in this case, the directions of exit air from the stationary and the moving blades are kept nearly the same as the design angle, because the flow passing through the stationary or the moving blades is forced to be deflected along their geometrical exit angles for any variable incidence angles. This means that $(\tan\alpha_{1m}+\tan\beta_{2m}$ in eq. (105) is kept constant for any off-design conditions and that is the same as the value at a design point, so that we can rewrite eq. (105) as

$$\Psi_m = K\Phi_m - 1 \tag{106}$$

where

$$K=\tan\alpha_{1m}+\tan\beta_{2m}=\text{const.} \tag{107}$$

The mean flow coefficient and mean loading coefficient at a design point are represented by Φ_m^* and Ψ_m^*, respectively.

$$\Psi_m^*=K\Phi_m^*-1 \tag{108}$$

From eqs. (106) and (108),

$$\frac{\Psi_m+1}{\Psi_m^*+1}=\frac{\Phi}{\Phi_m^*}=\left(\frac{C_{xm}}{C_{xm}^*}\right)\left(\frac{U_m^*}{U_m}\right) \tag{109}$$

$$\Psi_m=\left(\frac{C_{xm}}{C_{xm}^*}\right)\left(\frac{U_m^*}{U_m}\right)(\Psi_m^*+1)-1\,. \tag{110}$$

The indicated output of an air-turbine, through which G kg/s of air flows, can be represented from eqs. (102) and (103) by

$$L_{ti}=\frac{G\Delta L_{ti}}{102}=\frac{G}{102}\Psi_m\left(\frac{U_m^2}{g}\right)\quad\text{kW} \tag{111}$$

and at a design point, the indicated output L_{ti}^* of the same turbine, through which G^* kg/s of air flows, is represented by

$$L_{ti}^*=\frac{G^*}{102}\Psi_m^*\left(\frac{U_m^{*2}}{g}\right)\quad\text{kW}\,. \tag{112}$$

From eqs. (111) and (112),

$$L_{ti}=L_{ti}^*\left(\frac{G}{G^*}\right)\left(\frac{\Psi_m}{\Psi_m^*}\right)\left(\frac{U_m}{U_m^*}\right)^2. \tag{113}$$

In an air-turbine designed for axially leaving velocity

$$C_{xm}=k_1C_z\quad\text{and}\quad U_m=k_2C_z \tag{114}$$

where k_1 and k_2 are constants, *i.e.*, $k_1=1/\sqrt{3}$ and $k_2=(\tan\beta_{2m})/\sqrt{3}$.

Substituting these relations in eqs. (101) and (110), we obtain

$$\Phi_m=\Phi_m^*\,,\qquad \Psi_m=\Psi_m^* \tag{115}$$

and from eqs. (51) and (114)

$$\frac{G}{G^*}=\frac{\gamma aC_{xm}}{\gamma aC_{xm}^*}=\frac{C_z}{C_z^*}=\frac{N}{N^*} \tag{116}$$

where N is the rotational velocity of the rotor in RPM and

$$\frac{U_m}{U_m^*}=\frac{C_z}{C_z^*}=\frac{C_{xm}}{C_{xm}^*}=\frac{N}{N^*} \tag{117}$$

Substituting eqs. (115), (116) and (117) into eq. (113), the indicated output for any wind velocity C_z is given by

$$L_{ti}=L_{ti}^*(C_z/C_z^*)^3=L_{ti}^*(N/N^*)^3\,. \tag{118}$$

The same result can be also reduced from eqs. (48), (51) and (114) directly. The indicated torque can be obtained for any wind velocity by

$$T_i=T_i^*(C_z/C_z^*)^2=T_i^*(N/N^*)^2\,. \tag{119}$$

The total-to-total efficiency η_{TT} and the total-to-static efficiency η_{TS} are generally the function of Φ_m and Ψ_m, and it is apparent from eq. (115) that they will be nearly the same at any point on a curve passing through a design point and satisfying eq. (118).

This shows that a variable pitch mechanism will not be necessary for the wind air-turbine with stator to maintain high efficiency except that for maintaining constant speed or for feathering.

The brake torque T_e and the brake output at any off-design point can be calculated from eqs. (93) and (95).

9. Comparison between Air-Turbine with Stator and That without Stator

The most remarkable feature of the air-turbine described above is that it has a stator in front of a rotor. This blade arrangements (which is named here type-A) differs from the ordinary air-turbines without stator (type-B) in several points (Fig. 12).

Type-A has some merits and demerits compared with type-B. Type-A has a more complicated mechanism and greater weight and is more expensive

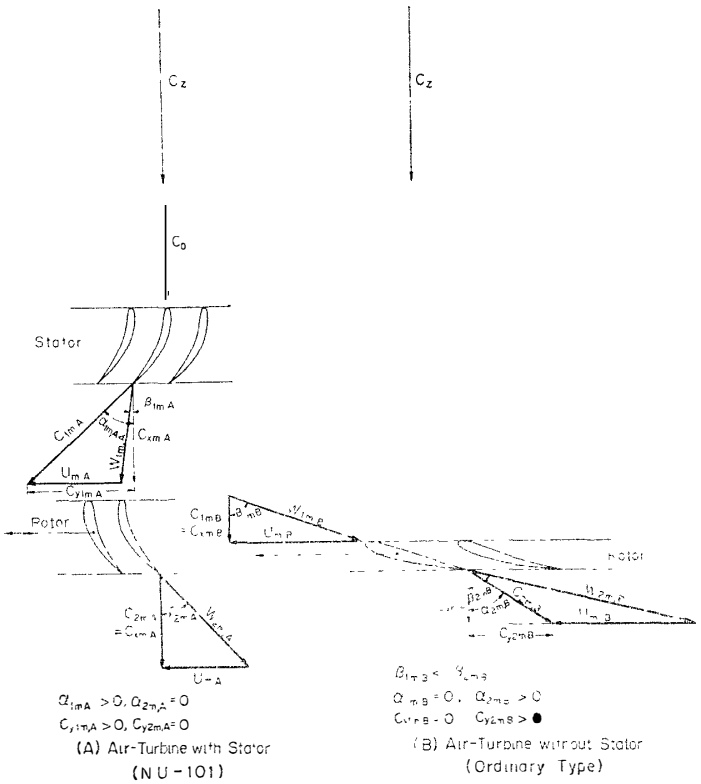

Fig. 12. Comparison between air-turbine with stator and that without stator.

than type-B. On the other hand, the output of type-A will be greater than that of type-B with the same external diameter under the same wind velocity.

As shown already in 4.8., the indicated output of type-A is given as follows:

$$(L_{ti})_A = \frac{\eta_{TT,A} G_A}{2000}\left[C_z^2 - C_{2m,A}^2\right] \quad \text{kW}$$

$$= \frac{T_{i,A}\omega_A}{102} = \frac{G_A}{102g} r_m C_{xm,A} \tan \alpha_{1m,A} \cdot \omega_A \tag{120}$$

where the weight flow rate of air, G_A, can be represented by

$$G_A = \gamma \alpha C_{xm,A} \quad \text{kg/s}. \tag{121}$$

For maximizing $(L_{ti})_A$, the axial velocity at mean radius must be chosen as

$$C_{xm,A} = C_z/\sqrt{3}.$$

The allowable maximum output for this mean axial velocity is

$$(L_{ti,\max})_A = \frac{\eta_{TT,A}}{1000}\left(\frac{\gamma a C_z^3}{3\sqrt{3}}\right) \quad \text{kW} \tag{122}$$

and the angular velocity ω_A can be obtained from eq. (120) as follows:

$$\omega_A = \frac{\eta_{TT,A} C_z}{\sqrt{3} r_m \tan \alpha_{1m,A}} \quad \text{rad/s}. \tag{123}$$

In the same way, the indicated output of type-B is given by

$$(L_{ti})_B = \frac{\eta_{TT,B} G_B}{2000}[C_z^2 - C_{2m,B}^2]$$

$$= \frac{T_{i,B}\omega_B}{102} = \frac{G_B}{102g} r_m C_{xm,B} \tan \alpha_{2m,B} \cdot \omega_B \tag{124}$$

where the weight flow rate of air can be represented by

$$G_B = \gamma a C_{xm,B} \quad \text{kg/s}. \tag{125}$$

From eqs. (124) and (125), we get

$$(L_{ti})_B = \frac{\eta_{TT,B}\gamma a}{2000} C_{xm,B}\left[C_z^2 - \left(\frac{C_{xm,B}}{\cos \alpha_{2m,B}}\right)^2\right] \tag{126}$$

For maximizing $(L_{ti})_B$, the mean axial velocity must be chosen as follows:

$$C_{xm,B} = C_z \cos \alpha_{2m,B}/\sqrt{3}. \tag{127}$$

Therefore, the mean exit absolute velocity is given by

$$C_{2m,B} = C_z/\sqrt{3} \tag{128}$$

and the maximum indicated output of type-B is represented as

$$(L_{ti,\max})_B = \frac{\eta_{TT,B}}{1000}\left(\frac{\gamma a C_z^3}{3\sqrt{3}}\right)\cos \alpha_{2m,B} \quad \text{kW}. \tag{129}$$

The angular velocity of type-B can be determined from eq. (124)

$$\omega_B = \frac{\eta_{TT,B} C_z}{\sqrt{3} r_m \sin \alpha_{2m,B}} = \frac{\eta_{TT,B} C_z}{\sqrt{3} r_m \tan \alpha_{2m,B} \cos \alpha_{2m,B}} \tag{130}$$

From eqs. (122) and (129), we get

$$\frac{(L_{tt,\max})_A}{(L_{tt,\max})_B} = \frac{\eta_{TT,A}}{\eta_{TT,B}\cos\alpha_{2m,B}} \tag{131}$$

and from eqs. (123) and (130)

$$\frac{\omega_A}{\omega_B} = \frac{\eta_{TT,A}\tan\alpha_{2m,B}}{\eta_{TT,B}\tan\alpha_{1m,A}}\cos\alpha_{2m,B} \tag{132}$$

If

$$\eta_{TT,A}=\eta_{TT,B} \quad \text{and} \quad \tan\alpha_{1m,A}=\tan\alpha_{2m,B}.$$

we get from eqs. (131) and (132),

$$\frac{(L_{tt,\max})_A}{(L_{tt,\max})_B} = \frac{1}{\cos\alpha_{2m,B}} > 1 \tag{133}$$

$$\frac{\omega_A}{\omega_B} = \cos\alpha_{2m,B} < 1 \tag{134}$$

Eqs. (133) and (134) show that the maximum output of type-A is usually greater than that of type-B even at a lower rotational speed than type-B.

For example, if the exit velocity angle of type-B is taken as $\alpha_{2m,B}=\alpha_{1m,A}=45°$, the power ratio becomes

$$(L_{tt,\max})_A/(L_{tt,\max})_B = \sqrt{2} \tag{135}$$

and the rotational speed ratio is

$$\omega_A/\omega_B = 1/\sqrt{2}. \tag{136}$$

Moreover, the lower speed of type-A in comparison with type-B results in lower stresses of rotor and lower frictional horsepower, although their frictional torques are the same. Accordingly, we can expect a higher net horsepower from type-A than type-B. In a real air-turbine, the total-to-total efficiency of type-B will be slightly greater than that of type-A, because it has no stator.

10. Details of Wind Electric Generator NU-101

The wind electric generator NU-101 comprises an axial flow air-turbine and a base box that contains (i) speed-up gear trains, (ii) a 2 kVA electric generator, and (iii) controlling and measuring instruments (refer to Figs. 1, 2 and 3).

Axial-flow air-turbine

External diameter	1,220 mm
Boss diameter	600 mm
Axial length (turbine only)	285 mm
Axial length (total)	1,245 mm
Weight (turbine only)	230 kgs

Stationary blades: built-up type of aluminium alloy cast blades.

Chord length	$l = 280$ mm
Axial chord	$b = 80$ mm

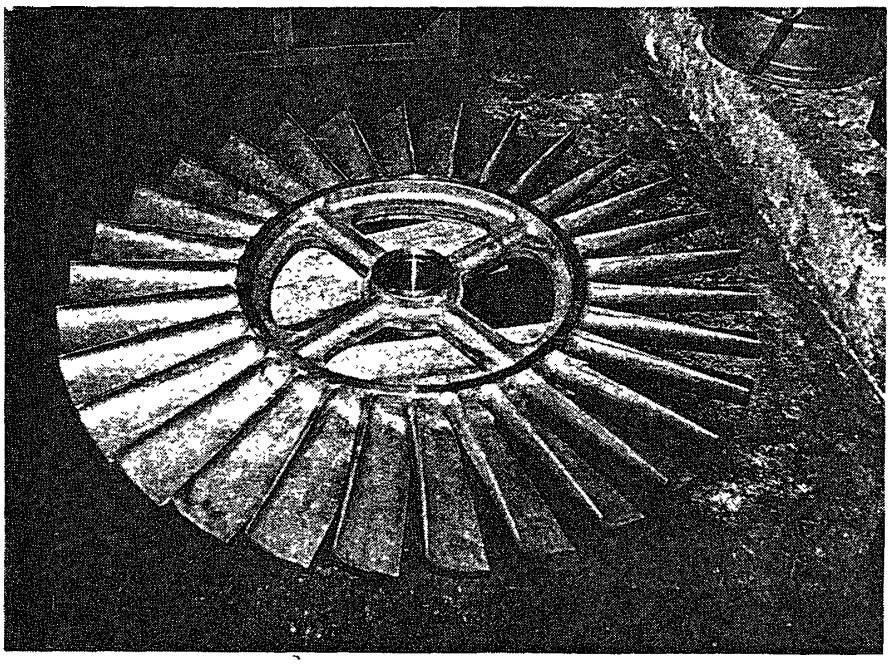

Fig. 13. Rotor of NU-101.

Spacing (at mean radius)	$S=97$ mm
Thickness ratio	$\delta/l=0.10$
Base profile	T6 with a parabolic camber line
Number of blades	31

Moving blades: cast in one body with an aluminium wheel (Fig. 13).

Chord length	$l=104$ mm
Axial chord	$b=71.5$ mm
Spacing (at mean radius)	$S=94$ mm
Thickness ratio	$\delta/l=0.10$
Base profile	T6 with a parabolic camber line
Number of blades	30

Base box

Steel framework. Stainless steel cover.

Dimensions $900\times760\times465$ (H) mm^3.

Weight 190 kg (inclusive of the following).

Speed-up gear trains

Two-stage gear trains driven by two synthetic rubber belts with teeth. Total speed ratio 6:1.

Electric generator

2 kVA, 100V, single phase AC.

DC self-exciting type with a variable resistance ($\leqq200\Omega$, 200W).

Meters

AC 300V voltmeter.

AC 30A ammeter.

Electronic over-run protector.

Base plate

Dimensions $1400\times700\times12$(t)

Weight 80 kg

As shown in Fig. 2, the base box is supported freely on a semi-circular base plate by a large ball bearing and two casters. The air-turbine and the base box are fixed tightly to each other, and can rotate around the ball bearing axis. The turbine can easily be manually set always in the wind direction. By adding a vertical stabilizer, the direction of the turbine axis can be automatically kept parallel to the wind direction.

Electronic over-run protector

The machine is provided with an over-run protector, which is useful in the case of blizzards. If the output voltage should exceed a preset value which can be selected freely between 110V and 130V, a shunt resistor is immediately bridged across the normal load by virtue of an electronic circuit, and the rotational speed is immediately suppressed.

11. Results of Test Runs in Tokyo and Syowa Station

The design of the wind electric generator NU-101 was started in May and completed in August 1972, by the present authors and their co-workers. This generator was constructed in only two months at a workshop of Nihon University

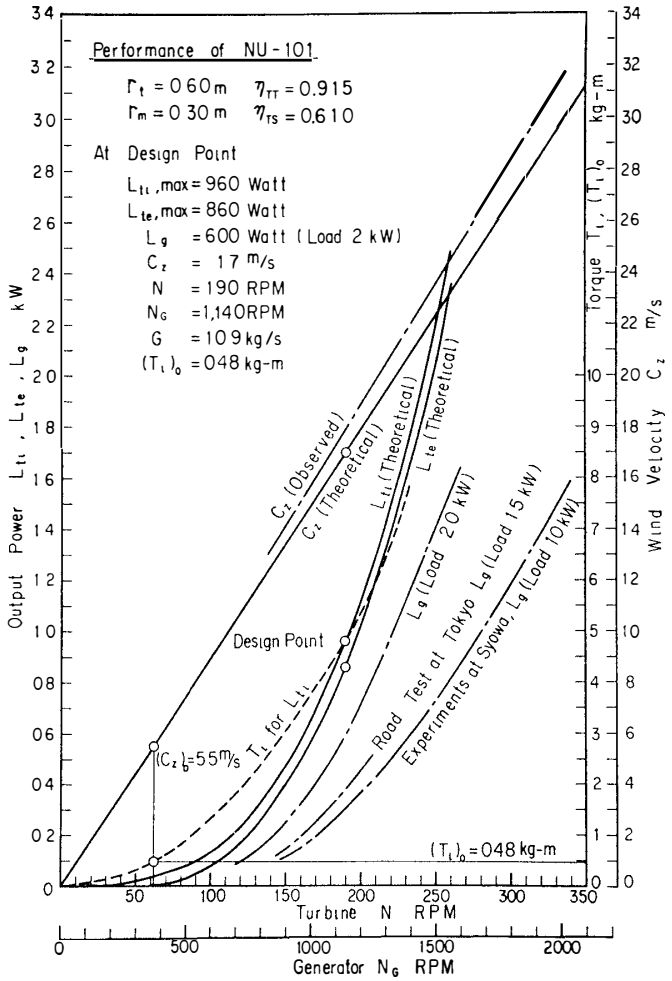

Fig. 14. Performance of NU-101, theoretically estimated and obtained by experiments.

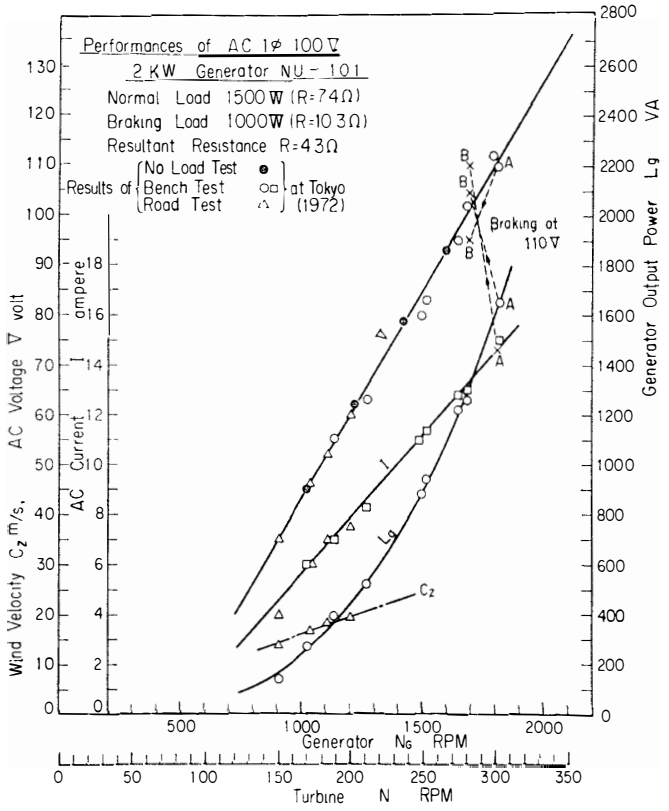

Fig. 15. Performance of NU-101 as deduced from running road test in Tokyo (Normal load 1.5 kW).

and forwarded on board the FUJI to Syowa on 17 November 1972 (JARE-14).

The authors did not have time to carry out a wind tunnel test before shipping. Instead, the machine was loaded on a light lorry, and its performance was examined at various speeds between 5.6 m/s and 19.4 m/s (20 and 70 km/h) by allowing the lorry to run on a straight test road. To eliminate natural wind effects on the speed, the lorry run back along the same path at the same speed.

Two pipe-heaters, 1.5 kW (7.4Ω) and 1.0 kW (10Ω) were submerged in water, to be used as the normal load and braking load, respectively.

The load system was so designed that the braking load was magnetically switched on in parallel with the normal load, the resulting resistance becoming 4.3Ω, when the turbine speed reached N = 300 RPM, and the output voltage became 110V.

The results of the test runs are summarized in Figs. 14 and 15. The wind air-turbine started to revolve at a wind speed of 5.5 m/s, where the indicated torque of the turbine became equal to the sum of the frictional torque T_f and the starting inertia torque $I_p(\omega/dt)$, which was 0.48 kg-m as predicted theoretically in Appendix.

The brake output of the wind air-turbine is given by eq. (95) and the net output of the electric generator may be given by

$$L_g = \eta_g L_{te} \tag{137}$$

where η_g is the generator efficiency.

The net output L_g of the NU-101 electric generator was 500W for a normal load of 1.5 kW pipe-heater (7.4Ω) at a wind speed of 19.4 m/s and the rotational speed of the turbine was 200 RPM. As the normal load, a 2.0 kW pipe-heater (5.0Ω) was used, L_g being increased to 700W (see Fig. 14).

The electrical braking circuit was switched on at a preset voltage 110V, corresponding to 300 RPM of the turbine speed (points A in Fig. 15) and the increased load suppressed the turbine speed to 285 RPM (point B in Fig. 15).

At Syowa Station, NU-101 was installed on top of a hill close to the buildings (Figs. 1 and 2). One of the authors, S. TAKEUCHI, a member of the 14th JARE made continuous observation of the rectified output voltage. One kW (10Ω) and 500W (20Ω) Nickel-Chrome electric resistors were employed as the normal and braking loads, respectively. The braking voltage was set at 130V. A part of the record for 5 April 1973, is shown in Fig. 16.

We can deduce the performance at Syowa Station of NU-101 by analyzing these records. The estimated performance has been summarized in Fig. 17 and Table 5. We learn from Figs. 16 and 17 that on 5 April 1973, the wind speed at Syowa Station ranged from 10 m/s to 32 m/s, and the corresponding variation in the rotational velocity ranged from 100 to 340 RPM and that the turbine speed was 182 RPM at 17 m/s.

The following remarks can be made on the basis of the experience at Syowa Station.

(1) No trouble caused by the turbine blades being coated with snow or frost has been experienced. However, in a blizzard, some snow entered the base box and froze the synthetic rubber belts. A planetary type gear box

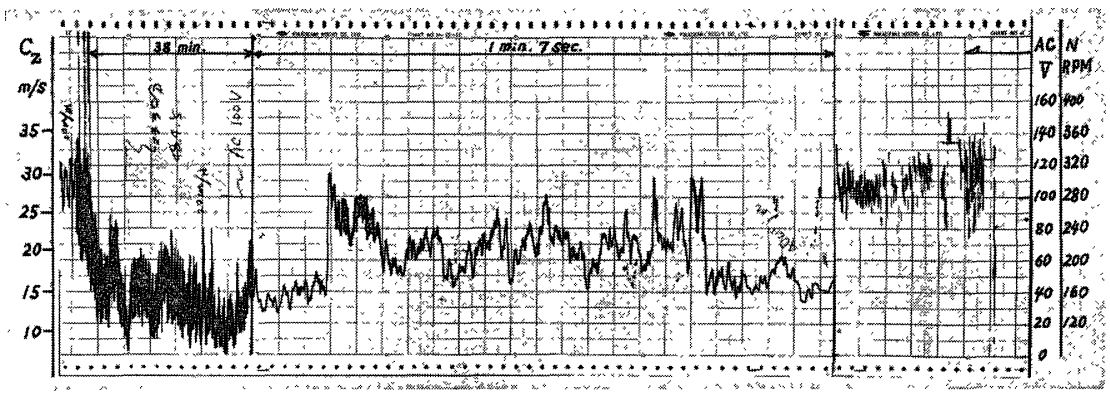

Fig. 16. Fluctuations in output voltage V, rotational velocity of turbine N and in wind velocity C_z (observation at Syowa Station on 5 April 1973).

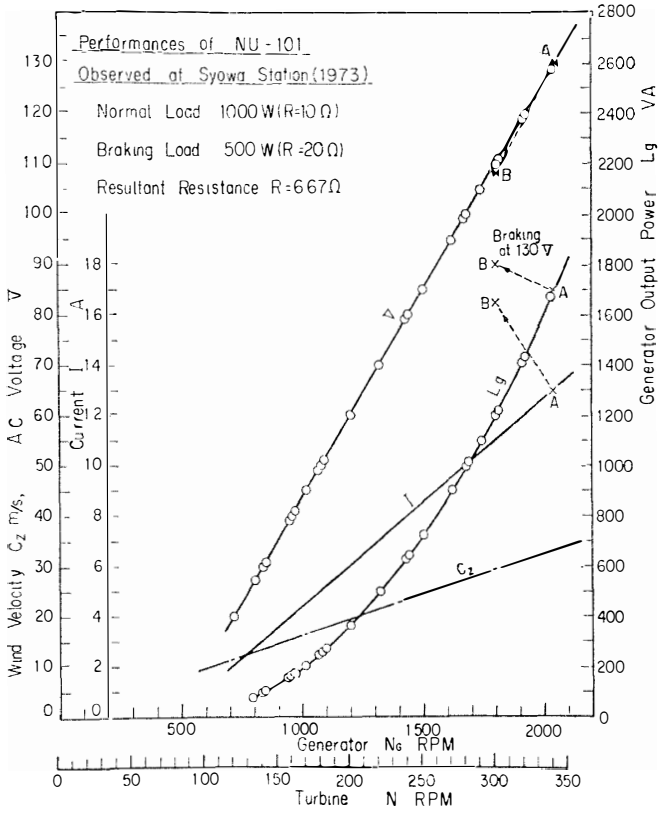

Fig. 17. Performance of NU-101 at Syowa Station (normal load 1 kW).

Table 5. The output performances of NU-101.

C_z (m/s)	N RPM	L_g Watt (Load 1 kW)	L_g Watt (Load 1.5 kW)	L_g Watt (Load 2 kW)	L_{te} Watt (Theoretical)*
15	158	150	200	310	470
17	182	240	330	480	700
20	207	410	520	800	1135
22.5	233	600	670	1150	1645
25	255	780	970	1550	2185
27.5	280	1030	1250	2000	2920
30	305	1280	1680	2530	3810
32.5	330	1580	2060	3125	4510

* Theoretically maximum value of L_{te} for $\eta_{TT}=0.915$.

directly connecting the turbine shaft to the generator (speed-up ratio 6:1 to 7:1) appears to be preferable to the belt-driven system.

(2) It has been established that the turbine can withstand violent blizzards up to 50 m/s. However, apprehension has been felt about the mounting of the base box to its base plate.

(3) The electrical braking system has proved to operate satisfactorily, although this system needs an over-sized generator. When the output voltage of the generator exceeds 130V, which was preset for 340 RPM of turbine speed, the electrical braking circuit was switched on automatically and the turbine speed was suppressed and the electric current was increased instantaneously as shown by dotted lines connecting A to B in Fig. 17.

(4) It would be worthwhile to try in the future a turbine whose blades as well as housing are made of reinforced plastics.

On the basis of our experience with NU-101, we are now designing an improved model, which will be designated as NU-102.

Acknowledgements

We should like to thank the members of JARE-14 for their cooperation in the test runs at Syowa Station and Messrs. R. OKAMOTO, S. OKUDA, and C. OZAWA, under-graduate students of the Mechanical Engineering Department, as well as the staff of the workshop of Nihon University for their cooperation in the design and construction of NU-101.

We are also deeply grateful for the financial aid by Nihon University.

References

ERYSON, F. E. (1974): Tilting at the energy crisis; A windmill on your roof. Machine Design, **40** (1), 20–25.

HORLOCK, J. H. (1966): Axial Flow Turbines. Butterworth, London, 275 pp.

JAPAN METEOROLOGICAL AGENCY (1971): Meteorological data at the Syowa Station in 1970. Antarctic Meteorol. Data, **11**, 151 pp.

MORIYA, T. and Y. TOMOSAWA (1961): The design and testing of wind power plants-design. United Nations Conference on New Sources of Energy, May 17, 1961, 1–8.

ROSEN, G., H. E. DEABLER and D. G. HALL (1975): Economic viability of large wind generator rotors. 10th Intersociety Energy Conversion Engineering Conference at University of Delaware, August 17–22, 1975, 1–6.

SACHS, P. (1964): Wind generation of electric power for radio-relay repeaters. Point to Point Telecommunications, **8** (2), 15–34.

SODERBERG, C. R. (1949): Unpublished notes, Gas Turbine Laboratory, Massachusetts Institute of Technology.

(Manuscript received October 13, 1975;
Revised manuscript received February 27, 1976)

APPENDIX

Detail of the Design of NU-101

An axial-flow air-turbine NU-101 was designed by the authors in 1972 on the basis of the theory described above. It has a stator with constant inlet and outlet angles along its radius and a rotor with moving blades, which have been designed on the basis of axially leaving velocity design.

(A) Indicated output at a design point

From the theoretical analysis described in 4.9., we adopted the design point of the air-turbine as follows:

atmospheric pressure at Syowa Station $P_z = 983.6$ mb (737.9 mm Hg)
atmospheric temperature $T_z = 262.5$ K
specific weight of air $\gamma = 1.307$ kg/m^3
wind speed at design point $C_z = 17$ m/s
total-to-total efficiency $\eta_{TT} = 0.915$ (at $t = -10.7$°C)
total-to-static efficiency $\eta_{TS} = 0.610$
(The estimation of efficiencies will be described in (D)).

The chief dimensions of the stator and the rotor were selected as follows:

tip radius of blades $r_t = 0.600$ m
hub radius of blades $r_h = 0.300$ m
mean radius of blades $r_m = 0.450$ m
blade height $H = r_t - r_h = 0.300$ m
annulus area $a = \pi(r_t^2 - r_h^2) = 0.848$ m^2

We may find by the use of Table 1 that

ideal specific output $e_0 = 1.222 \times (1.307/1.293) = 1.235$ kW/m^2
specific weight flow rate of air $(G/a) = 12.69 \times (1.307/1.293) = 12.83$ kg/s.m^2

Accordingly, the indicated output L_{ti} and the weight flow rate of air G at the design point are evaluated as follows:

$$L_{ti} = \eta_{TT} a e_0 = 0.915 \times 0.848 \times 1.235 = 0.96\text{kW}$$
$$G = a(G/a) = 0.848 \times 12.83 = 10.9 \text{ kg/s}.$$

The total energy generated by NU-101 yearly at Syowa Station can be evaluated from Table 3 as

$$\sum_{C_z}(E_0/a) = 1958 \text{ kWh/y.m}^2$$

The total indicated energy that is available yearly is estimated as

$$E=\eta_{TT}a\sum_{Cz}(E_0/a)=0.915\times0.848\times1958=1520\ \text{kWh/y}\ .$$

It is to be noted that the indicated output and the total energy can be obtained when the mean axial velocity C_{xm} of the air-turbine is taken as

$$C_{xm}=C_z/\sqrt{3}=17/\sqrt{3}=9.82\ \text{m/s}\ .$$

(B) Static pressure P_0 and total pressure P_0*

The dynamic head of the wind can be calculated as

$$\gamma C_z^2/2g=1.307\times(17^2/2\times9.8)=19.27\ \text{mm}\ H_2O\ (1.42\ \text{mmHg})\ ,$$

$$\gamma C_0^2/2g=1.307\times(9.82^2/2\times9.8)=6.43\ \text{mm}H_2O\ (0.47\ \text{mmHg})\ ,$$

and accordingly the static pressure rise in front of the stator is

$$P_0-P_z=(\gamma C_z^2/2g)-(\gamma C_0^2/2g)=12.8\ \text{mm}\ H_2O(0.95\ \text{mmHg})\ .$$

The total pressure at (Z) and (0) in Fig. 5 can be calculated by eq. (19).

$$P_z{}^*=P_0{}^*=P_z+(\gamma C_z^2/2g)=737.9+1.42=739.3\ \text{mmHg}\ .$$

(C) Estimation of velocity triangles

(C-1) Velocity triangles at hub radius r_h

In the design of NU-101, a pure impulse stage is adopted at its hub radius and the degree of reaction increases with radius r.

Hence, the following relations must hold at the hub radius r_h:

$$P_{1h}=P_z+\Delta P_{rel}{}^*\fallingdotseq P_z$$

$$C_{1h}=\varphi_s C_z\fallingdotseq C_z=17\ \text{m/s}$$

$$W_{1h}=W_{2h}$$

The air stream flowing into an air-turbine is directed axially, so that the inlet angle α_0 is zero at any radius of the stationary blades. For $r_m/r_h=0.450/0.300=1.5$, we find in Table 4 that the outlet angle from the stationary blades is $\alpha_1=45°$.

Hence, the axial velocity at the hub radius, C_{xh}, is

$$C_{xh}=C_{1h}\cos\alpha_1=17/\sqrt{2}=12.0\ \text{m/s}\ .$$

On the other hand, it follows from Fig. 18 (A) that

$$2U_h=C_{1h}\sin\alpha_1=17/\sqrt{2}=12.0\ \text{m/s}\ .$$

so that,

$$U_h=6.0\ \text{m/s}$$

where U_h is the peripheral velocity at the hub radius r_h. The angular velocity of the rotor can be determined as

$$\omega=U_h/r_h=6.0/0.300=20\ \text{rad/s}.$$

The rotational speed of the turbine is

$$N=60\omega/2\pi=190\ \text{RPM}.$$

Referring to Fig. 18 (A), the relative inlet and outlet velocities of the rotor, W_{1h} and W_{2h}, are given by

$$W_{1h}=W_{2h}=\sqrt{C_{xh}{}^2+U_h{}^2}=\sqrt{12.0^2+6.0^2}=13.4\ \text{m/s}\ .$$

The velocity angle β_{1h} between W_{1h} and the x-axis and that β_{2h} between W_{2h} and the x-axis, are given by

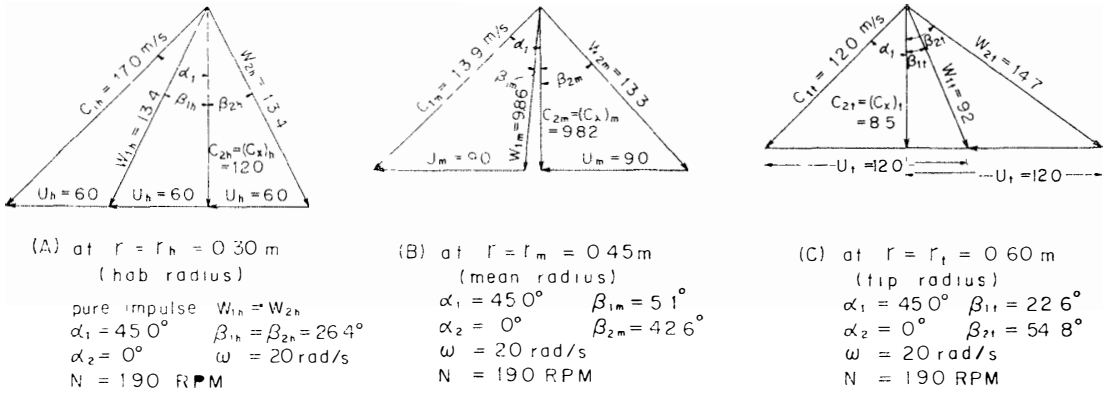

Fig. 18. Velocity triangles for NU-101.

$$\cos\beta_{1h}=C_{xh}/W_{1h}=12.0/13.4=0.896,\quad \beta_{1h}=26.4^\circ$$
$$\cos\beta_{2h}=C_{xh}/W_{2h}=12.0/13.4=0.896,\quad \beta_{2h}=26.4^\circ.$$

The velocity triangle at the hub radius is given in Fig. 18 (A).

(*C-2*) *Velocity triangle at the mean radius* r_m

From eq. (86), we obtain the following relations

$$C_{1h}=K_1(\mathrm{cosec}\,\alpha_1)\,r_h^{-\sin^2\alpha_1}$$
$$C_{1m}=K_1(\mathrm{cosec}\,\alpha_1)\,r_m^{-\sin^2\alpha_1}$$

and hence,

$$C_{1m}=C_{1h}(r_m/r_h)^{-\sin^2\alpha_1}=17.0(0.45/0.300)^{-1/2}=13.9\ \mathrm{m/s}$$
$$C_{xm}=C_0=9.82\ \mathrm{m/s}.$$
$$U_m=r_m\omega=0.450\times 20=9.0\ \mathrm{m/s}$$

From Fig. 18 (B), the relative velocities W_{1m} and W_{2m} at the mean radius can be calculated by

$$W_{1m}=\sqrt{C_{1m}^2+U_m^2-2C_{1m}U_m\sin\alpha_1}=9.86\ \mathrm{m/s}$$
$$W_{2m}=\sqrt{C_{2m}^2+U_m^2}=13.3\ \mathrm{m/s},$$

and the angles β_{1m} and β_{2m} are given by

$$\cos\beta_{1m}=C_{xm}/W_{1m}=9.82/9.86=0.996,\quad \beta_{1m}=5.1^\circ$$
$$\cos\beta_{2m}=C_{xm}/W_{2m}=9.82/13.3=0.736,\quad \beta_{2m}=42.6^\circ$$

The velocity triangle at the mean radius is shown in Fig. 18 (B).

(*C-3*) *Velocity triangle at the tip radius* r_t

In the same way for the mean radius, the velocities and their angles can be determined as follows:

$$C_{1t}=C_{1h}(r_t/r_h)^{-\sin^2\alpha_1}=17.0(0.600/0.300)^{-1/2}=12.0\ \mathrm{m/s}$$
$$C_{xt}=C_{xh}(r_t/r_h)^{-\sin^2\alpha_1}=12.0(0.600/0.300)^{-1/2}=8.5\ \mathrm{m/s}$$
$$U_t=r_t\omega=0.600\times 20=12.0\ \mathrm{m/s}$$
$$W_{1t}=\sqrt{C_{1t}^2+U_t^2-2C_{1t}U_t\sin\alpha_1}=9.2\ \mathrm{m/s}$$
$$W_{2t}=\sqrt{C_{xt}^2+U_t^2}=14.7\ \mathrm{m/s}$$
$$\cos\beta_{1t}=C_{xt}/W_{1t}=0.923,\quad \beta_{1t}=22.6^\circ$$
$$\cos\beta_{2t}=C_{xt}/W_{2t}=0.577,\quad \beta_{2t}=54.8^\circ.$$

The velocity triangle at the tip radius is shown in Fig. 18 (C).

(D) Evaluation of blade losses and turbine efficiencies

The dimensions of the stationary and moving blades are determined as given in article 10.

The kinematic viscosities of air can be calculated by eq. (73).

$\nu = 0.042 \times 10^{-4}$ m/s^2 for $t = -10.7$°C (at Syowa)

$\nu = 0.273 \times 10^{-4}$ m/s^2 for $t = 15$°C (at Tokyo).

The loss coefficients of air-turbine set at Syowa Station are estimated as follows:

Stator deflection angle of the stationary blades

$$\varepsilon_s = \alpha_0 + \alpha_1 = 0^\circ + 45^\circ = 45^\circ$$

Reynolds number obtained from eq. (71) is

$$R_h = 3.5 \times 10^5$$

and the loss coefficients of the stationary blades are given by eqs. (68) and (69),

$$\hat{\xi}_s' = 0.065\,, \qquad \hat{\xi}_s = 0.044\,.$$

Rotor deflection angle of the moving blades

$$\varepsilon_m = \beta_{1m} + \beta_{2m} = 5.1^\circ + 42.6^\circ = 47.7^\circ$$

Reynolds number obtained from eq. (72) is

$$R_h = 3.6 \times 10^5$$

and the loss coefficients are

$$\hat{\xi}_m' = 0.067\,, \qquad \hat{\xi}_m = 0.044\,.$$

The total-to-total efficiency η_{TT} and the total-to-static efficiency η_{TS} of NU-101 can be estimated as,

$$\hat{\xi}_s C_{1m}^2 + \hat{\xi}_m W_{2m}^2 = (0.044 \times 13.9^2) + (0.044 \times 13.3^2)$$
$$= 8.5 + 7.8 = 16.3 \text{ m}^2/\text{s}^2$$
$$C_z^2 - C_{2m}^2 = 17^2 - 9.82^2 = 193 \text{ m}^2/\text{s}^2$$

From eq. (64), $\zeta = 16.3/(193 - 16.3) = 0.093$

The total-to-total efficiency of NU-101 at Syowa Station is estimated by eq. (63)

$$\eta_{TT} = 1/(1+\zeta) = 1/(1+0.093) = 0.915$$

From eq. (44), the total-to-static efficiency of NU-101 is

$$\eta_{TS} = \eta_{TT}[1 - (C_{2m}/C_z)^2] = 0.915[1 - (9.82/17)^2] = 0.610\,.$$

These turbine efficiencies will be realized at low air temperature in Syowa Station, but they will be lowered slightly at high temperatures such as those in Tokyo because of the increased loss coefficients due to the increasing kinematic viscosity of air. The loss coefficients and turbine efficiencies at Tokyo are estimated as follows:

The loss coefficient of the stationary blades is

$$\hat{\xi}_s = 0.070 \quad \text{for} \quad R_h = 0.54 \times 10^5$$

and the loss coefficient of the moving blades is

$$\hat{\xi}_m = 0.072 \quad \text{for} \quad R_h = 0.55 \times 10^5\,.$$

The total-to-total efficiency and the total-to-static efficiency of the same turbine at Tokyo are

$$\eta_{TT} = 0.865 \quad \text{for} \quad \zeta = 0.157$$

and

$\eta_{TS}=0.567$

It is to be noted that the temperature effects on flow-losses and on turbine efficiencies cannot be ignored, especially in the Antarctic, where the air temperature is very low.

(E) Calculation of the indicated output power from the velocity triangle at mean radius

The indicated output can be determined approximately from the velocity triangle at the mean radius as follows:

$C_z=17$ m/s, $N=190$ RPM, $G=10.9$ kg/s.

From Fig. 18 (B), the inlet and outlet absolute velocities for the moving blades are

$C_{1m}=13.9$ m/s, $C_{2m}=C_{xm}=9.82$ m/s.

The angle between the absolute velocity vector C_{1m} and x-axis and that between C_{2m} and x-axis are

$\alpha_{1m}=45°$, $\alpha_{2m}=0°$.

From eq. (92), the indicated torque

$$T_i=\frac{G}{g}(C_{1m}\sin\alpha_{1m}+C_{2m}\sin\alpha_{2m})r_m$$
$$=\frac{10.9}{9.8}(13.9/\sqrt{2})\times 0.450$$
$$=4.9 \text{ kg.m.}$$

From eq. (94), the indicated output power of NU-101

$L_{ti}=2\pi NT_i/6120=2\pi\times 190\times 4.9/6120=0.96$ kW.

From eq. (96), the total-to-static efficiency

$\eta_{TS}=2000(L_{ti}/C_z^2G)=2000(0.96/17^2\times 10.9)=0.61$.

(F) Evaluation of the starting torque

From experiments in Tokyo, we know that the turbine rotor of NU-101 starts to run when $(C_z)_0=5.5$ m/s.

the annulus area of NU-101 $a=0.848$ m^2

the specific weight of air $\gamma=1.22$ kg/m^3 (at Tokyo)

the starting torque $(T_i)_0$ of NU-101 can be estimated by eq. (100).

$$(T_i)_0=T_f+I_p\frac{d\omega}{dt}=\frac{\gamma a(C_z)_0^2}{3g}(\tan\alpha_{1m}+\tan\alpha_{2m})r_m$$
$$=\frac{1.22\times 0.848\times 5.5^2\times 0.450}{3\times 9.8}=0.48 \text{ kg.m.}$$

This result coincides with the experimental result as shown in Fig. 14.

(G) Off-design performance

The performance of NU-101 at the design point is given as follows,

$C_z^*=17$ m/s

$T_i^*=4.9$ kg.m, $T_f=0.48\fallingdotseq 0.5$ kg.m, $T_e^*=4.4$ kg.m.

$L_{ti}^*=0.96$ kW, $L_f^*=0.10$ kW, $L_{te}^*=0.86$ kW

where T_f and L_f^* are the friction torque and the friction power at the design point. As shown above,

$U_m^*=9.0$ m/s, $C_{xm}^*=9.82$ m/s, $G^*=10.9$ kg/s.

The performance at any wind speed of C_z can be estimated by using the eqs. (116)-(119), (93) and (95).

As an example, the highest attainable performance of NU-101 at the wind velocity of $C_z=20.6$ m/s is estimated as follows:

rotational speed	$N=N^*(C_z/C_z^*)=190(20.6/17)=230$ RPM
weight flow rate of air	$G=G^*(C_z/C_z^*)=10.9(20.6/17)=13.2$ kg/s
indicated output	$L_{ti}=L_{ti}^*(C_z/C_z^*)^3=0.96(20.6/17)^3=1.7$ kW
indicated torque	$T_{ti}=T_{ti}^*(C_z/C_z^*)^2=4.9(20.6/17)^2=7.2$ kg.m
brake torque	$T_{te}=T_{ti}-T_f=7.2-0.5=6.7$ kg.m
brake output	$L_{te}=2\pi NT_{te}/6120=2\pi\times230\times6.7/6120$ $=1.6$ kW

The theoretical performance curves for NU-101 estimated by the method described above are shown in Fig. 14.